BMC Biology

RESEARCH ARTICLE

Open Access

PmLBD3 links auxin and brassinosteroid signalling pathways on dwarfism in *Prunus mume*

Yufan Ma[1†], Chengdong Ma[1†], Pengyu Zhou[1], Feng Gao[1], Wei Tan[1], Xiao Huang[1], Yang Bai[1], Minglu Li[1], Ziqi Wang[1], Faisal Hayat[2], Ting Shi[1], Zhaojun Ni[1] and Zhihong Gao[1*]

Abstract

Background Grafting with dwarf rootstock is an efficient method to control plant height in fruit production. However, the molecular mechanism remains unclear. Our previous study showed that plants with *Prunus mume* (mume) rootstock exhibited a considerable reduction in plant height, internode length, and number of nodes compared with *Prunus persica* (peach) rootstock. The present study aimed to investigate the mechanism behind the regulation of plant height by mume rootstocks through transcriptomic and metabolomic analyses with two grafting combinations, 'Longyan/Mume' and 'Longyan/Peach'.

Results There was a significant decrease in brassinolide levels in plants that were grafted onto mume rootstocks. Plant hormone signal transduction and brassinolide production metabolism gene expression also changed significantly. Flavonoid levels, amino acid and fatty acid metabolites, and energy metabolism in dwarf plants decreased. There was a notable upregulation of *PmLBD3* gene expression in plant specimens that were subjected to grafting onto mume rootstocks. Auxin signalling cues promoted *PmARF3* transcription, which directly controlled this upregulation. Through its binding to *PmBAS1* and *PmSAUR36a* gene promoters, *PmLBD3* promoted endogenous brassinolide inactivation and inhibited cell proliferation.

Conclusions Auxin signalling and brassinolide levels are linked by *PmLBD3*. Our findings showed that *PmLBD3* is a key transcription factor that regulates the balance of hormones through the auxin and brassinolide signalling pathways and causes dwarf plants in stone fruits.

Keywords Prunus mume, Grafting, Hormonal signalling, Dwarfing mechanism

Background

The height of plants is a significant characteristic of fruit tree cultivation, and the cultivation of dwarf crops is generally associated with more condensed plant structures, as well as increased yield and improved quality. Consequently, dwarf plants play a crucial role in the advancement of fruit tree breeding and production methodologies [1]. The phenomenon of plant dwarfing, which occurs as a result of material flow and hormonal interactions between the rootstock and scion following grafting [2], has consistently been a subject of concern and a significant approach in the breeding of dwarf crops

†Yufan Ma and Chengdong Ma contributed equally to this work.

*Correspondence:
Zhihong Gao
gaozhihong@njau.edu.cn
[1] Laboratory of Fruit Tree Biotechnology, College of Horticulture, Nanjing Agricultural University, Nanjing, Jiangsu, China
[2] College of Horticulture, Zhongkai University of Agriculture and Engineering, Guangzhou, Guangdong, China

and the selection of varieties. *Prunus mume* (mume) is an important crop of stone fruit originating from China. In contrast to fruit trees, such as apples and peaches, mume exhibits a diminished stature and is more suited for contemporary orchard cultivation practices that emphasise compact planting arrangements. Previous research has demonstrated that scions grafted onto mume rootstocks exhibit notable dwarfing characteristics, with a shorter length and reduced plant height compared to those grafted onto *Prunus persica* (peach) rootstocks [2]. However, the precise molecular mechanism by which mume rootstocks exert control over plant dwarfing remains elusive and requires further investigation.

Plant hormones, known as signalling molecules, play a crucial role in the regulation of plant growth. They can control several aspects of vegetative and reproductive growth in grafted plants, both in terms of timing and spatial distribution. The effect of dwarfing rootstocks on scions is often reflected in changes in the scion hormone content [3–6]. In addition, rootstocks can affect gene expression levels in scions, indicating that related genes may be involved in the molecular mechanism of rootstock dwarfing [3, 6–9]. The expression patterns of genes involved in hormone metabolism and transduction in the rootstock may induce stunted growth of the scion and alter the concentrations of certain endogenous hormones in the scion [10, 11].

Auxin, a vital endogenous hormone in plants, plays a direct role in various physiological processes, including cell elongation and embryogenesis [12]. The regulation of indole-3-acetic acid (IAA) on plant height is accomplished by the synergistic interaction of many variables. In early research, Michalczuk found that the IAA content in apple dwarfing rootstocks was significantly lower than that in tree rootstocks [13]. Subsequent investigations have also demonstrated a significant reduction in the expression level of auxin production genes in dwarfed rootstocks compared to arborescent rootstocks [14]. Plants overexpressing auxin response factor *OsARF19* exhibit dwarfing, narrow leaves, and increased leaf angle [15]. Small auxin-up RNA (SAUR) is a crucial gene family involved in the early response to auxin. While SAUR is known to play a significant role in auxin-induced plant growth, it can also be regulated by different hormone pathways and transcription factors that are independent of auxin [16]. In *Arabidopsis*, the majority of SAUR genes are believed to facilitate plant growth by stimulating cell elongation, particularly in leaves, stems, and flower organs [17–22]. Brassinosteroids (BRs) are well recognised as crucial hormones in the regulation of plant height. To date, extensive research has been conducted on the biosynthesis, catabolism, and signalling pathways of BRs in plants, leading to a comprehensive understanding of these processes [23–25]. Moreover, the mechanisms by which genes involved in these pathways influence plant height have been elucidated to a considerable extent. In a general sense, mutation genes responsible for the biosynthesis of BRs or overexpression of genes involved in the catabolism of BRs can result in a reduction in plant height [26, 27]. In addition, mutations in regulatory factors that govern BRs signalling pathways can give rise to dwarf phenotypes characterised by BRs insensitivity [28–30]. In general, the regulatory effect of BRs on plant height is frequently contingent on their interplay with other plant hormones, governing cell elongation and plant growth through an intricate network of hormonal interactions [15, 24, 31, 32]. However, the mechanisms by which other plant hormones, such as auxin signalling, regulate the synthesis and metabolism of BRs remain unclear.

Lateral organ boundaries domains (LBDs) are specific transcription factors in plants characterised by the presence of the lateral organ boundaries (LOB) domain. The LBD gene family is comprised of a substantial number of members and mainly functions in the regulation of growth, development, and stress response [33, 34]. In *Arabidopsis thaliana* (Arabidopsis), LBD6 positively regulates gibberellin production, while LBD40 inhibits it [35, 36]. *AtLOB* regulates the BRs metabolic genes, enabling *AtBAS1* to exert an inhibitory effect, thereby reducing BRs accumulation and lateral organ growth [37]. Abscisic acid inhibited the expression of β-glucuronidase (GUS) induced by LBD14 in Arabidopsis, altering the transcriptional activity of LBD14 in roots [38]. LBD18 affects the transcriptional activity of auxin response factor (ARF) genes, such ARF7 and ARF19, by binding the Phonx and Bem1 domains [39]. These findings demonstrate the existence of a comprehensive and intricate regulatory association between the LBD protein and plant hormones. Overexpression of the LBD gene leads to dwarfism in plants [40, 41], but the regulatory mechanism is not clear.

This study examined the growth of the scion variety 'Longan' grafted onto mume and peach rootstocks. Mume rootstocks reduced the plant height, internode length, and node number. The transcriptome and metabolome of plants from two grafting combinations were analysed. The changes in gene transcription levels and metabolites in dwarfed plants produced by mume rootstock grafting helped explain plant dwarfing caused by rootstock scion contact. Among the 13 differentially expressed genes (DEGs) of the LBD family identified in the transcriptome, *PmLBD3* stood out as being significantly differentially expressed in multiple tissues simultaneously, with higher expression levels observed throughout the entire plant. This suggests that *PmLBD3*

may play a crucial role among the homologous genes of the LBD family in inducing dwarfing in mume rootstock. Plant height, internode length, and cell size decreased significantly when *PmLBD3* was overexpressed. *PmLBD3* overexpression increased gibberellic acid (GA_3) and decreased IAA and brassinolide (BL). The binding of *PmARF3* to the *PmLBD3* promoter increased its expression, according to subsequent research. In turn, *PmLBD3* triggered the subsequent production of *PmBAS1* and negatively regulated the activity of *PmSAUR36a* genes, which govern plant height by modulating the quantity of endogenous hormones and cell expansion. We concluded that *PmLBD3* controlled plant height by integrating the auxin and BL metabolic pathways via the ARF-LBD-BAS1 and SAUR36 cascade regulation mechanisms. The findings support a comprehensive understanding of auxin and BL interactions and identify the *PmLBD3* gene as a key regulator of endogenous plant hormone levels and plant stature.

Results

Prunus mume rootstocks cause scion dwarfing by altering growth hormones

In contrast to peach rootstock 'Zhongtaokangzhen No.1' (ZTKZ), mume rootstock 'Lve' (LVE) exerted a substantial influence on the vertical stature of mume scion 'Longyan' plants that were grafted (Fig. 1a). Following the process of grafting, notable variations in the length, diameter, internode length, and number of primary stems could be observed across distinct rootstocks as the plant undergoes growth. The scion of 'Lonyan' grafted onto mume rootstocks exhibited reduced plant height, a lower number of nodes, and a shorter internode length compared to those grafted onto peach rootstocks (Fig. 1b–e). To further clarify the dwarfing effect of mume rootstocks on scions, we grafted peach scion 'Hujingmilu' onto mume and peach rootstocks and compared their growth conditions (Additional file 1: Fig. S1a–d). The results showed that the mume rootstock had the same inhibitory effect on the growth of peach scions, indicating that it could be used as a dwarfing rootstock for further research. Subsequent studies have used the grafted plants of the scion 'Lonyan' as materials.

The BL content in the stems and leaves of the mume rootstock plant was notably lower than that of the peach rootstock (Fig. 1f). Furthermore, there was no statistically significant difference in the levels of IAA and GA_3 between the two groups (Additional file 1: Fig. S2a, b). These findings suggest that the difference in BL content may potentially account for the occurrence of scion dwarfing. This study revealed that the roots of grafted mume rootstocks had higher levels of BL compared to peach rootstocks. After comparing the root hormone content of non-grafted rootstocks with grafted plants under similar growth conditions, grafting did not impact the BL content in rootstock roots. However, there was a reduction in the gibberellin content in both mume and peach rootstocks after grafting (Additional file 1: Fig. S2c, d). To ascertain the potential correlation between scion dwarfing and the absence of growth hormones, we conducted measurements on the length of scions after BL application on the mume and peach rootstock plants that were grafted. The application of hormone treatment effectively reversed the stunted growth of the mume rootstock plants (Fig. 1g, h). However, the same hormone concentration did not have a significant effect on the growth of scions on peach rootstocks (Fig. 1g). In comparison to the peach rootstocks that were not subjected to treatment, the group that received treatment with mume rootstocks had phenotypic characteristics that were comparable to those observed in peach rootstock plants (Fig. 1g, h). Treatment with BL at the same concentration did not significantly enhance the growth of peach rootstock plants. This suggests that the endogenous hormone levels in peach rootstock plants were in an optimal state, with no apparent hormone deficiency.

(See figure on next page.)

Fig. 1 'Longan' grafted on mume and peach rootstocks demonstrates distinct growth states. **a** Different 'Longyan/Peach' (LP) and 'Longyan/Mume' (LM) grafting phenotypes. Scale bars = 25 cm. **b**–**e** The growth level of plants after grafting was monitored by measuring at 10-day intervals, starting from 75 days after grafting. The data presented in this study represent the average ± standard error (SE) of eight biological replicates ($n = 8$). **b** Primary shoot length. **c** Internodal length. **d** Trunk diameter of the scion. **e** Number of nodes. **f** Amount of BL in the two grafting pairs was measured. The BL values are the average standard error of three biological replicates ($n = 3$). **g** The effects of BL treatments on the growth of mume and peach rootstocks. Anova was used to identify significance tests between datasets: $^{*}P < 0.05$, $^{**}P < 0.01$, $^{***}P < 0.0001$. Following a grafting period of 75 days, mume rootstock plants were subjected to treatments of 0.5 mg/L BL and water at 10-day intervals. The treated plants were then compared to both untreated mume and peach rootstock plants. **h** Grafted plants treated with BL and without hormones were measured for primary shoot length, internodal length, and number of nodes. The data presented reflects the average value ± SE obtained from 8 independent biological replicates ($n = 8$). The presence of an asterisk in the datasets signifies a statistically significant difference, as determined by the Student's *t*-test ($^{*}P < 0.05$, $^{**}P < 0.01$, $^{***}P < 0.0001$). 'ns' denotes the absence of a statistically significant difference. Supporting data for individual data values in the figure legend are shown in Additional file 3

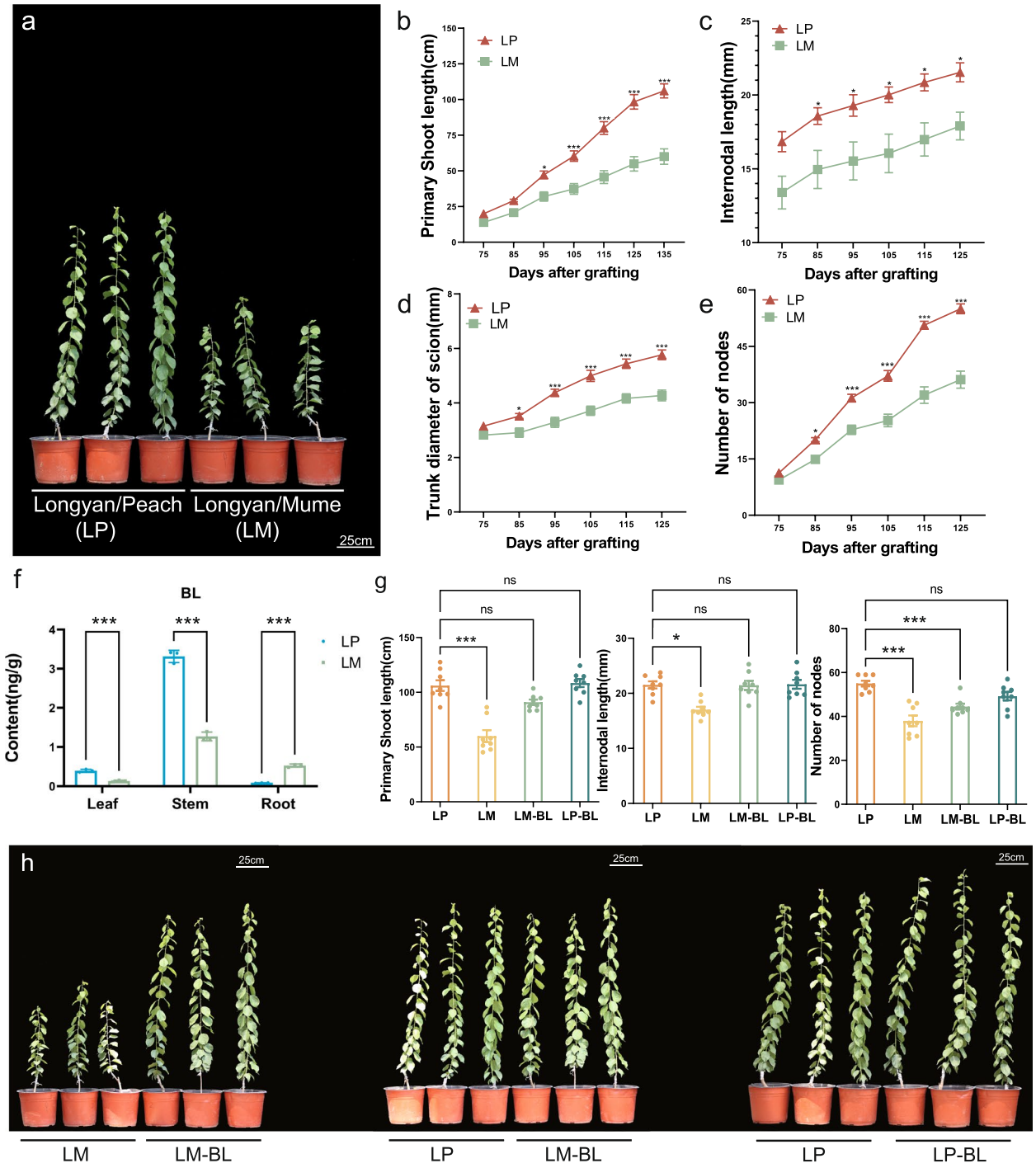

Fig. 1 (See legend on previous page.)

These findings also suggest that grafting with mume rootstock may suppress BL levels in plants.

Cytological investigations were performed on the stem tissue sections of scions subjected to grafting using mume and peach rootstocks. Mume rootstocks exhibited a thinner phloem in the stem compared to peach rootstocks. This was attributed to the presence of fewer layers of phloem cells and a more compact arrangement of these cells, resulting in smaller intercellular gaps. Additionally, the xylem ducts in mume rootstocks were relatively narrower, with a reduced number of cells surrounding the ducts and a smaller overall volume. These

observations are supported by Additional file 1: Fig. S1e, f (depicting the phloem) and g, h (depicting the xylem ducts). Xylem ducts are responsible for transporting water and inorganic salts absorbed by the roots to the upper part of the plant. Narrower ducts affect the transport efficiency of water and inorganic substances in the plant, thus affecting the plant development process [42]. Overall, the results indicate that the mume rootstock may induce plant dwarfing by reducing the endogenous BL content in the scion through material exchange between the rootstock and the scion.

Changes in transcriptome and metabolome patterns between scions after grafting on different rootstocks

To gain insights into the alterations in gene expression patterns among scions grafted onto distinct rootstocks, we conducted transcriptome sequencing analyses on several plant tissues, including leaves (L), stems (S), grafting interfaces (G), and roots (R), of plants grafted onto rootstocks of peach and mume varieties. In this study, we examined the variations in gene expression between various tissues in peach ('Longyan/Peach', LP) and mume rootstock scion plants ('Longyan/Mume', LM). We employed a significance threshold of $P < 0.05$ and $|\log_2 \text{FC (fold change)}| \geq 1$ as the criteria for identifying DEGs. A total of 3500, 4156, 3450, 4749, and 191 DEGs were discovered across the five comparable groups, namely LM-G/LM-S, LM-G/LP-G, LM-L/LP-L, LP-G/LP-S, and LM-S/LP-S, respectively, following the grafting procedure (Fig. 2a). To assess the validity of the transcriptome data, six differentially expressed genes were chosen at random for quantitative real-time polymerase chain reaction (qRT-PCR) analysis. The findings from this analysis demonstrated consistent gene expression patterns, confirming the dependability of the transcriptome data (Additional file 1: Fig. S3). Upset results of DEGs between different tissues showed that most of the DEGs in the stem and grafting interface were the same between the

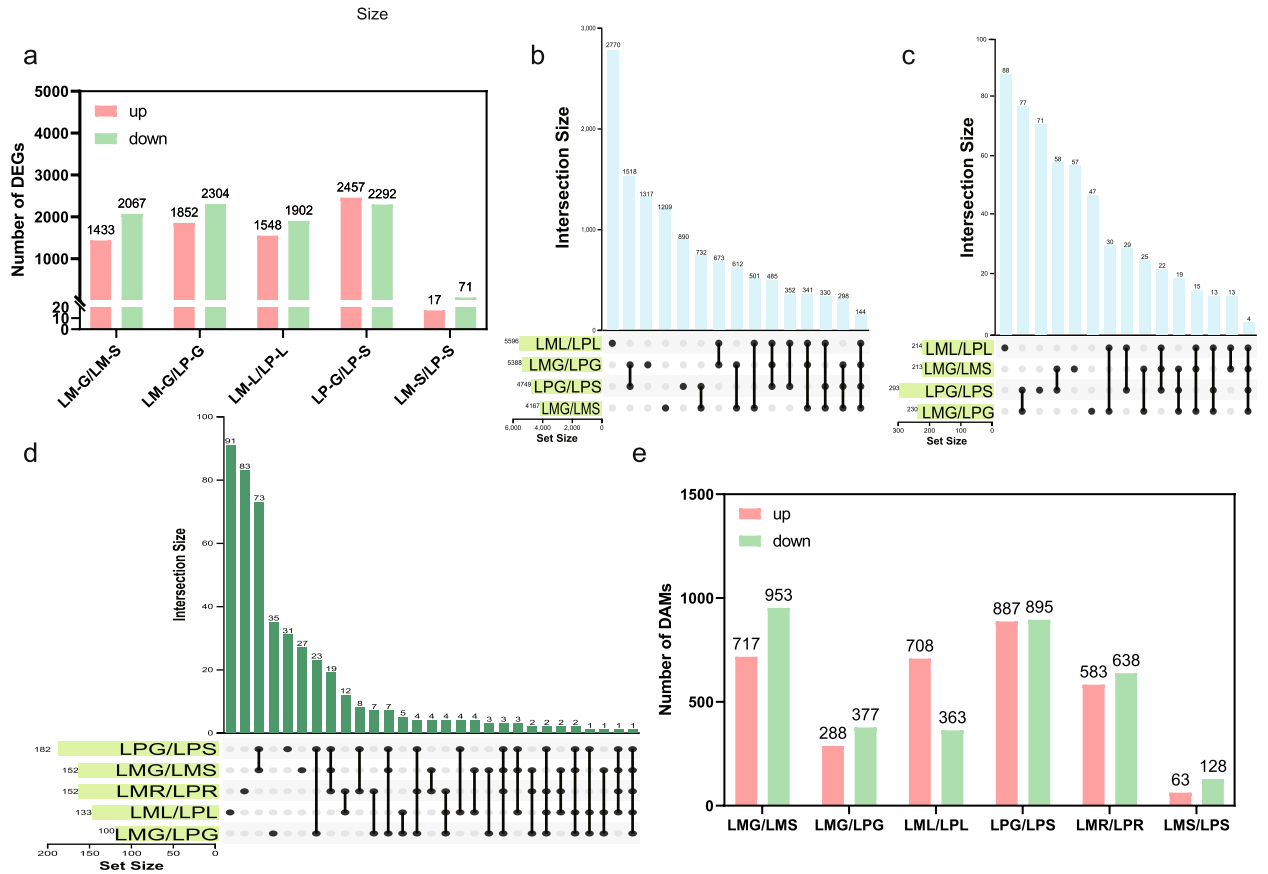

Fig. 2 Changes in transcription and metabolism in plants with different rootstock and scion combinations. **a** Histogram showing the distribution of DEGs. The comparison groups are LM-G/LM-S, LM-G/LP-G, LM-L/LP-L, LP-G/LP-S, and LM-S/LP-S. Red represents upregulated DEGs, and green represents downregulated DEGs. **b** Upset Venn plot of DEGs overlap between different tissues after grafting peach and mume rootstocks. **c** Upset Venn plot of differentially expressed transcription factors in different comparison groups. **d** Upset Venn plot of differentially expressed metabolites between different comparison groups after grafting. **e** Histogram showing the distribution of DAMs. The comparison groups are LM-G/LM-S, LM-G/LP-G, LM-L/LP-L, LP-G/LP-S, LM-R/LP-R, and LM-S/LP-S. Red represents upregulated DAMs, and green represents downregulated DAMs

two grafting combinations, and only a small part of these DEGs were significantly different in leaves (Fig. 2b). This suggests that the expression patterns regulated by grafting in the leaves differed from those observed between the stems and grafting interfaces. The statistical analysis of differentially expressed transcription factors also revealed a consistent pattern. When comparing LM-G/LM-S and LP-G/LP-S, certain genes showed differential expression in the grafting interface and stem of the mume rootstock scion, while no significant difference was observed in the tissues of the peach rootstock scion. This suggests that these genes are strongly influenced by the mume rootstock and may play a role in the mechanism of rootstock–scion interaction (Fig. 2c).

Liquid chromatography-tandem mass spectrometry (LC–MS/MS) equipment was employed to quantify metabolite concentrations in various regions of the grafted plants. Additionally, metabolomics analysis was carried out. In the leaves, stems, and roots, 4159, 5582, and 3682 metabolites, respectively, were detected. The screening process for identifying significant differential accumulated metabolites (DAMs) involved using a set of criteria: VIP ≥ 1, FC ≥ 1.2 or ≤ 0.83, and q value < 0.05. Orthogonal partial least squares discriminant analysis (OPLS-DA) revealed a notable distinction among the samples belonging to the various comparison groups. Moreover, all samples fell within the 95% confidence interval (Additional file 1: Fig. S4). Venn analysis was conducted on the DAMs annotated within the metabolic pathway across various groups. Only a few metabolite species in the leaves and roots were consistent with the differential profile observed in stems (Fig. 2d). This suggests notable disparities in the metabolic profiles of plant roots and leaves compared to stems. The scion leaves of mume rootstocks exhibited a predominance of upregulated DAMs, whereas in other tissues, the DAMs in the stem, root, and grafting interfaces of mume rootstock plants were predominantly downregulated compared to peach rootstock-grafted plants (Fig. 2e). The potential cause for this phenomenon could be attributed to the grafting procedure impeding the movement and transfer of substances inside the roots, stems, and leaves, thereby exerting an influence on the overall plant growth.

The auxin and BL pathways are important for controlling the size of scions

To gain a deeper comprehension of the impact of mume rootstocks on hormone equilibrium in scions throughout the grafting process, additional examination was undertaken on DEGs identified through transcriptome screening. The gene function of DEGs caused by the interaction between rootstocks and scions was determined by Gene Ontology (GO) enrichment analysis. Significant enrichment of GO pathways associated with photosynthesis, including photosystem I and photosynthesis, was observed in the three control groups: LM-G/LM-S, LP-G/LP-S, and LM-L/LP-L. The investigation of the interaction between rootstocks and scions on the functioning of leaf genes, hormone response, auxin-activated signalling pathway, cellular response to auxin stimulation, transporter activity, naringenin chalcone synthesis activity, flavonoid biosynthesis and metabolism, and auxin efflux revealed a significant enrichment of these processes in the GO terms. This implies that the modulation of hormones and metabolites, such as auxin and flavonoids, could potentially play a role in the development of dwarfing during the leaf response mechanism. Furthermore, within the comparison group between grafting interfaces, a greater number of DEGs were associated with the process of membrane construction. The auxin-activated signalling route and the cellular response to auxin signalling exhibited considerable enrichment in all comparison groups. This suggests that the main DEGs involved in controlling graft dwarfing may be associated with hormone-signalling pathways, including auxin (Fig. 3a).

To have a deeper understanding of the molecular mechanism behind the interaction between rootstock and scions, and its impact on plant growth, we performed Kyoto Encyclopedia of Genes and Genomes (KEGG) annotation and enrichment analysis on DEGs identified from the transcriptome data. Metabolic pathways associated with plant hormones exhibited significant enrichment in various comparison groups, including plant hormone signal transduction, BL biosynthesis, and flavonoid biosynthesis. This observation suggests that alterations in these genes potentially govern physiological changes in plants during the interaction between rootstocks and scions (Fig. 3b). Through the examination of the interconnectedness among enrichment pathways and the construction of a network diagram (Fig. 3c), it was evident that the BL production pathway was linked to many KEGG pathways related to metabolism and hormones. These associations have a notable influence on the growth process of the scion. The observed decline in BL levels in mume rootstock scions (Fig. 1f) and the findings from transcriptome differential expression gene analysis suggest that auxin signal transduction and BL biosynthesis pathways play a crucial role in determining the height of scions following grafting. KEGG gene function annotation revealed DEGs in the BL biosynthesis pathway, which were then statistically analysed and heat-mapped. More DEGs were annotated as CYP734A1/BAS1, and their expression levels were increased in mume rootstock plants (Fig. 3d). Among the available reports, the BAS1 gene is responsible for the

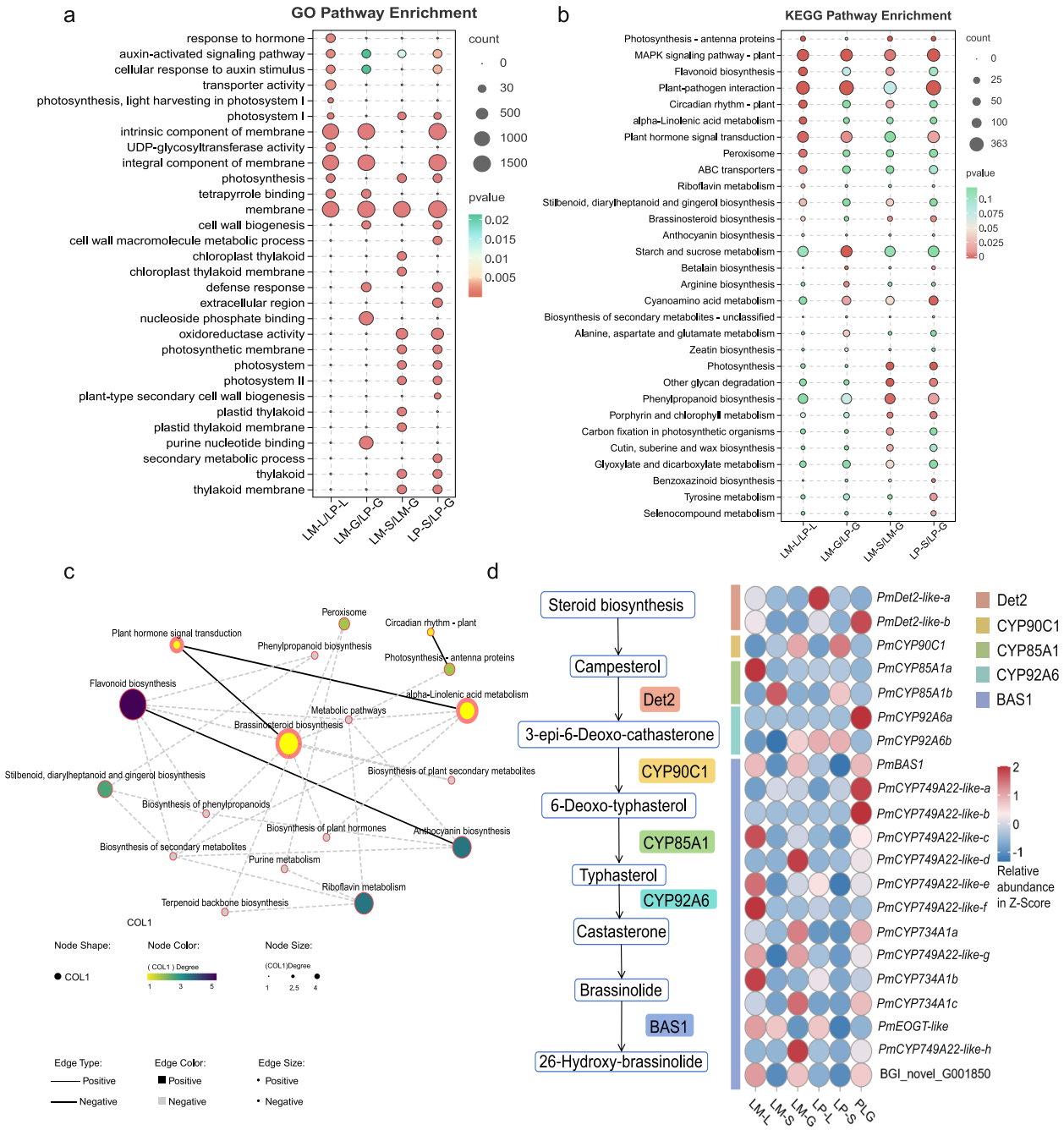

Fig. 3 The auxin and brassinolide pathways regulate scion size. **a** GO enrichment of DEGs between different tissues. **b** KEGG enrichment of DEGs between different tissues. **c** A correlation network diagram depicting the relationships between KEGG-enriched pathways. The KEGG pathways are visually represented by nodes that vary in colour and size. The size of each node corresponds to the number of genes that have been enriched in the respective pathway through KEGG enrichment analysis. The gradient colours of the nodes indicate the *P* value obtained from KEGG enrichment analysis. Additionally, pathways supplemented from the KEGG connection database are represented by grey nodes. The links between pathways are represented by solid lines, while the linkages between complementary routes and input pathways are represented by dashed lines. **d** A *Z*-score was used to normalise the rows, and heat maps showed the difference in expression of brassinolide biosynthesis pathway DEGs in different tissues

direct inactivation of BL in plants [37], which may affect scion growth and development. This indicates that the use of mume rootstock grafting has a greater effect on BL metabolism. Among the DEGs annotated as CYP734A1/BAS1, the gene with the highest gene expression level was named *PmBAS1* (Additional file 2: Table S1). Based on these results, *PmBAS1* may be the key gene affecting BL content in dwarfing scions.

Combined metabolomic and transcriptomic analysis

Based on data from the KEGG database, the metabolic pathways of DAMs in various plant tissue parts were analysed to observe changes in metabolites in stunted plants after grafting. Enrichment analysis indicated that DAMs in scion leaves grafted onto mume rootstock, compared to peach rootstock, were notably enriched in linoleic acid metabolism, biosynthesis of unsaturated fatty acids, biosynthesis of amino acids, carbon fixation in photosynthetic organisms, and alanine, aspartate, and glutamate metabolism. Metabolites, such as linoleic acid, palmitic acid, citric acid, and succinic acid, increased, while fructose and sucrose decreased. In the stem, DAMs were significantly enriched in oxidative phosphorylation, biosynthesis of amino acids, biosynthesis of secondary metabolites, and the pentose phosphate pathway, with most DAMs showing decreased content, suggesting restricted energy metabolism in dwarf scion stems. DAMs in the grafting interface and root were enriched in flavonoid biosynthesis and secondary metabolite biosynthesis pathways, with flavonoid DAMs downregulated in plants using a mume rootstock (Fig. 4a, Additional file 2: Table S2). The flavonoid content in the roots of mume rootstock was lower, impacting the metabolic substance content at the grafting interface and subsequently influencing the growth and metabolism of the scion in the upper part of the plant. This suggests that inhibiting flavonoid synthesis could be a method for dwarfing the scions of mume rootstock. By combining the findings of previous transcriptome analysis and hormone assays, the insufficiency of BL and flavonoid metabolites in plants utilising mume as rootstock might be a crucial factor restricting plant growth.

In our previous transcriptome analysis, significant changes were observed in the expression patterns of BAS1 genes in the scions of mume rootstocks, which may explain the decrease in the endogenous BL content in plants (Fig. 3d). Research on *Arabidopsis* suggests that the *AtBAS1* gene is directly regulated by the LBD family transcription factor *AtLOB* [37]. Within transcriptome analysis, 29 genes with LOB domains were identified, with 13 LBDs showing differential expression. These genes were labelled based on their chromosomal localisation sequence (Additional file 1: Fig. S5a), and a Venn diagram was constructed. *PmLBD3* exhibited differential expression in the leaves, grafting interfaces, and roots of both graft combinations simultaneously (Additional file 1: Fig. S5b). Specifically, *PmLBD3* expression was notably increased in mume rootstock plants after grafting (Additional file 2: Table S3). It is hypothesised that *PmLBD3* plays a role in regulating BL metabolism in mume rootstock scions, potentially serving as a key gene in facilitating this process. To investigate this hypothesis, the expression abundance of *PmLBD3* in the transcriptome was analysed alongside metabolome data. The findings revealed a significant correlation between *PmLBD3* and the DAMs in important metabolic pathways, such as flavonoid biosynthesis and carbohydrate metabolism, across various tissues (Fig. 4b–d). The involvement of *PmLBD3* in regulating metabolic substance content in grafted dwarfed plants suggests a potential link to the scion stunting process induced by the mume rootstock. It is possible that *PmLBD3* influences the hormone content to contribute to the stunting process.

PmLBD3 is involved in the auxin signal transduction pathway and reduces the active BL content

To establish the regulatory association between *PmLBD3* and *PmBAS1*, we conducted yeast one-hybrid (Y1H) assays. The experimental findings indicate that *PmLBD3* exhibits a direct binding affinity towards the promoters of *PmBAS1* (Fig. 5a). A double luciferase reporter gene assay was conducted in tobacco plants to investigate their regulatory capacity. The interaction between *PmLBD3* and the *PmBAS1* promoter enhanced its transcriptional regulation (Fig. 5b). Furthermore, the JASPAR website was utilised to predict the binding site of *PmLBD3* to the promoter. Subsequently, electrophoretic mobility shift assay (EMSA) was employed to ascertain the physical binding of the recombinant protein His-*PmLBD3* to the predicted binding motif within the deoxyribonucleic acid (DNA) probe's *PmBAS1* promoter regions. The mobility of the His-*PmLBD3* protein experienced modification when it interacted with the probe. Moreover, the gradual increase in the concentration of the cold probe led to a decline in the interaction between the labelled probe and the His-*PmLBD3* protein (Fig. 5c). The experimental results suggest that *PmLBD3* can engage directly and specifically with the promoters of *PmBAS1* in an in vitro environment. The aforementioned findings suggest that *PmLBD3* has the ability to directly enhance *PmBAS1* expression through its binding to the promoter region.

To verify whether changes in the expression level of the *PmLBD3* gene were related to the transmission of plant hormone signals, qRT-PCR was employed to assess the expression level of *PmLBD3* in mume-grafted plants following hormone treatment. The findings of

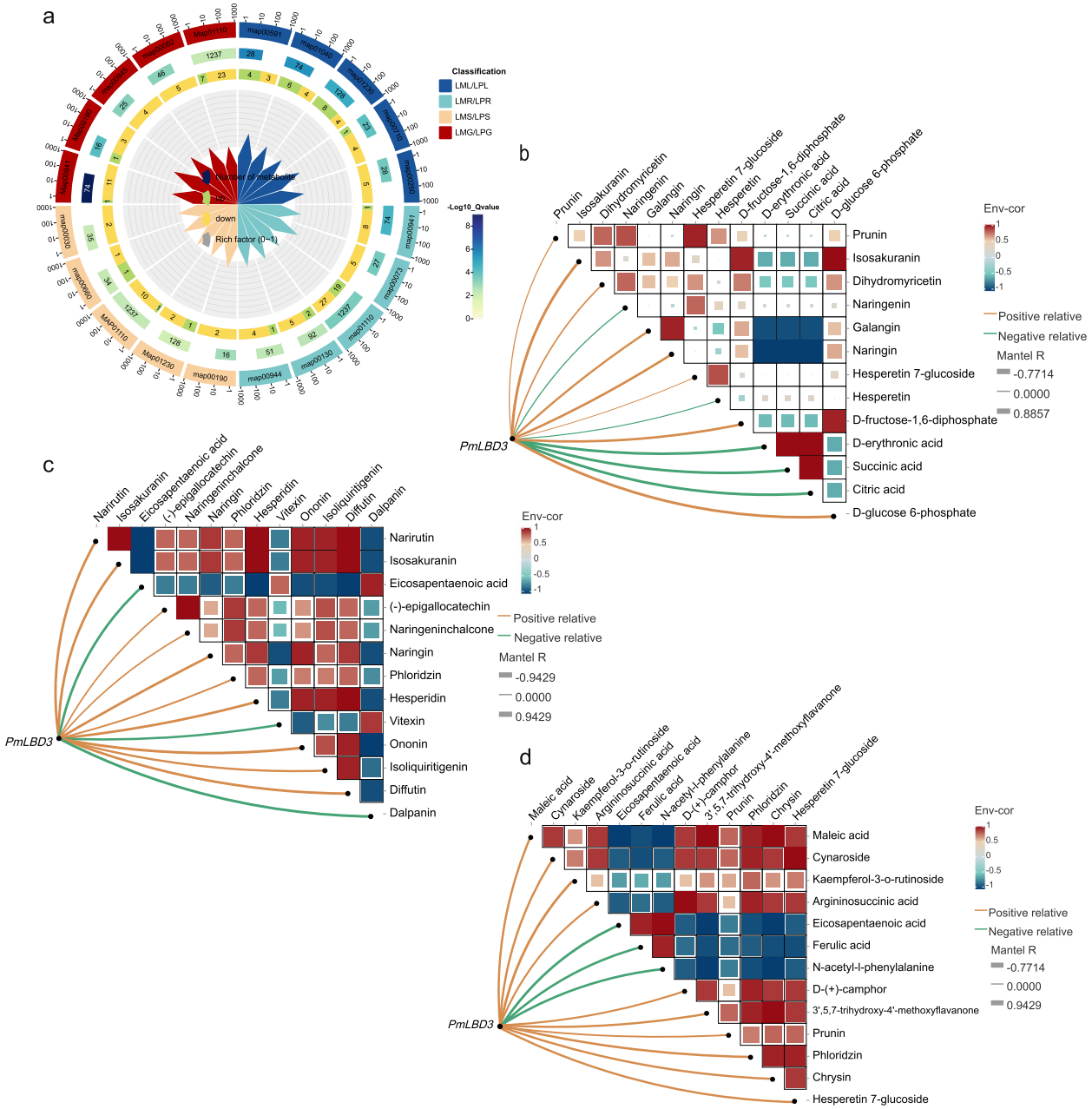

Fig. 4 Analysis of both the metabolome and the transcripts. **a** Enrichment analysis of the KEGG pathway for differentially expressed metabolites in different comparison groups after grafting. The enrichment of divergent metabolites in the leaves, roots, stems, and grafting interfaces of the two rootstock plants is shown by four distinct hues. The initial circle visually represents the five most prominent KEGG pathways. The second circle in the visual representation signifies the quantity of metabolites within the metabolic family, as well as the *P* value denoting the level of enrichment of metabolites in the KEGG pathway. The third circle illustrates the regulation of metabolites that have been enriched, with the colour yellow representing downregulation and green representing upregulation. The fourth circle symbolises the enrichment variables associated with each KEGG pathway. To obtain comprehensive information regarding the KEGG pathways, please consult Additional file 2: Table S2. **b** Correlation analysis between the abundance of *PmLBD3* transcriptome genes and differentially expressed metabolites in the leaves of different grafted plants ($n=6$). **c** Correlation analysis between the abundance of *PmLBD3* transcriptome genes and differentially expressed metabolites in the roots of different grafted plants ($n=6$). **d** Correlation analysis between the abundance of *PmLBD3* transcriptome genes and differentially expressed metabolites in the stems of different grafted plants ($n=6$)

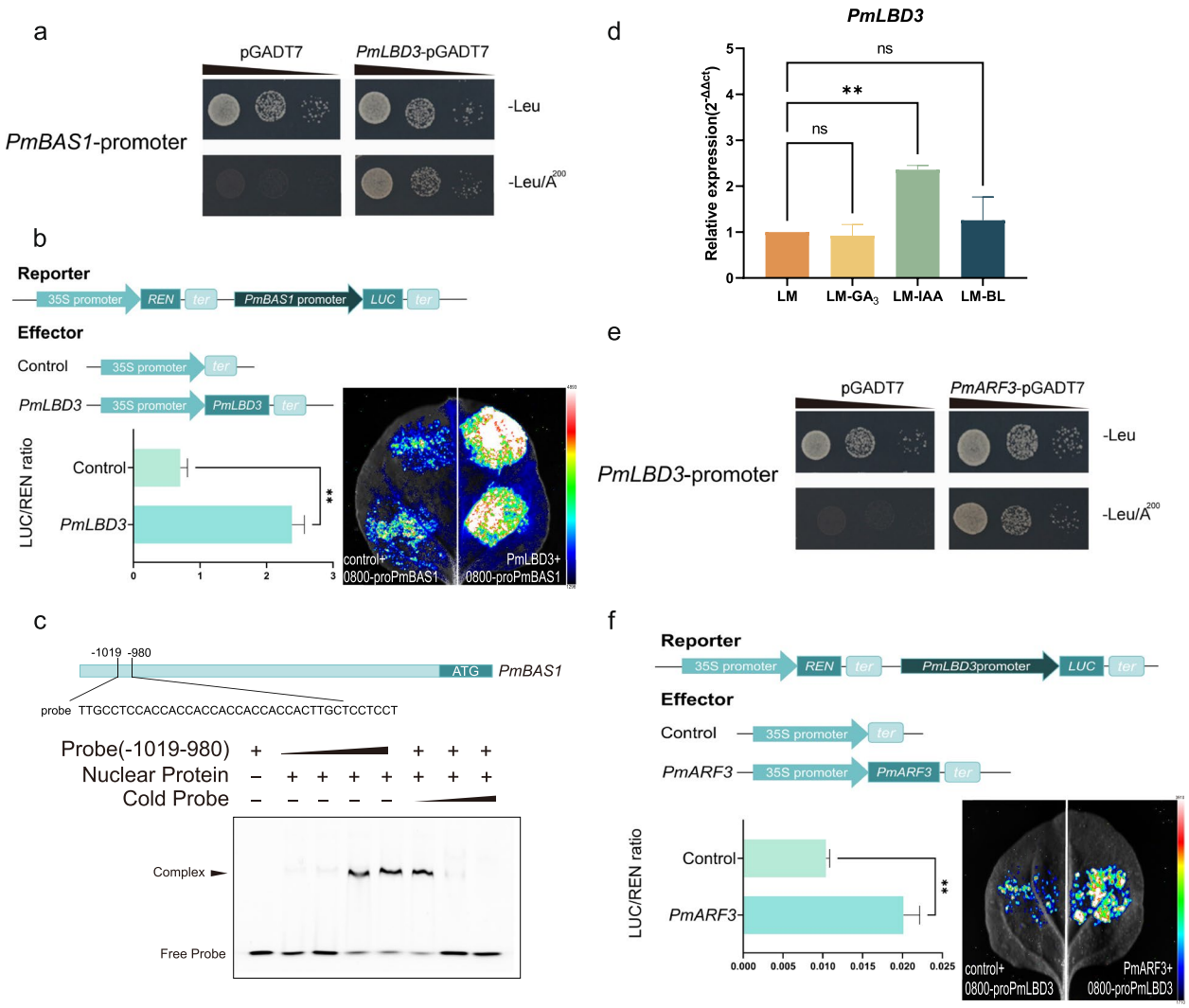

Fig. 5 *PmLBD3* is regulated by *PmARF3* and regulates the *PmBAS1* transcript levels. **a** Interactions of *PmLBD3* with *PmBAS1* promoters were detected in Y1H. -Leu stands for a culture medium without leucine, while -Leu.^{200} stands for a culture medium without leucine with 200 ng/mL of AbA. PGADT7 represents the negative control. **b** A double luciferase assay was used to detect the regulation of *PmLBD3* on the *PmBAS1* promoter. **c** His-*PmLBD3* recombinant protein can bind to specific DNA fragments in the *PmBAS1* promoter regions. DNA probes labelled with 5′ FAM. Use identical but unlabelled DNA fragments (cold probes) as competitors. **d** After treatment with water, IAA, GA_3, and BL, the expression of the *PmLBD3* gene in leaves was detected by qRT-PCR. The qRT-PCR experiment analysed three biological replicates ($n=3$). The primer sequences used for qRT-PCR are shown in Additional file 2: Table S4. The presence of an asterisk in the datasets signifies a statistically significant difference, as determined by the Student's *t*-test (*$P<0.05$, **$P<0.01$). **e** Interactions of *PmARF3* with *PmLBD3* promoters were detected in Y1H. **f** A double luciferase assay was used to detect the regulation of *PmARF3* on the *PmLBD3* promoter. **b**, **f** The negative control is the empty vector, and the data are shown as the mean ± SE ($n=3$). Student's test identified significant differences from the control (**$P<0.01$). A CCD imaging system collected the luminescence photos, and the pseudo colour bar indicates the intensity range. Supporting data for individual data values in the figure legend are shown in Additional file 3

this study indicate that *PmLBD3* upregulation can be achieved by auxin application (Fig. 5d). Analysis of the *PmLBD3* promoter revealed that it contained a TGT CTC AuxRE motif related to the auxin-responsive factor ARF gene. It was hypothesised that genes involved in auxin signal transduction could control *PmLBD3* transcription.

A set of five ARF family transcription factors exhibiting differential expression in the transcriptome were cloned and submitted to a Y1H test. The purpose of this experiment was to determine whether these ARF transcription factors possessed the ability to bind to ARF-responsive sites present in the *PmLBD3* promoter. *PmARF3* exhibited direct binding affinity towards the AuxRE

motif (TGTCTC) present in the *PmLBD3* promoter (Fig. 5e, Additional file 1: Fig. S6a). The findings from the dual luciferase reporter gene experiment showed that *PmARF3* exerted a positive regulatory effect on the transcription of *PmLBD3*, leading to an elevation in its expression level (Fig. 5f).

PmLBD3 overexpression reduces plant height and affects the plant hormone balance and cell expansion

With the goal of having a deeper understanding of the role of *PmLBD3* in the regulation of plant growth and development, we created transgenic tobacco plants overexpressing *PmLBD3* under the control of the 35S CaMV promoter. Subsequently, we identified three overexpressing lines (*OE29*, *OE30*, *OE55*) and used empty vector plants as controls for subsequent analysis (Fig. 6a). Tobacco overexpression resulted in notable stunting throughout its entire growth cycle, characterised by a substantial decrease in internode length and an increase in stem thickness (Fig. 6b). The plant heights of the *OE29*, *OE30*, and *OE55* strains exhibited a reduction of 85.35, 84.85, and 87.63%, respectively, in comparison to the plant heights of empty vectors. Additionally, the stem thickness of these strains demonstrated an increase of 75.01, 19.56, and 12.75%, respectively (Fig. 6c, d). Furthermore, the overexpressing strain demonstrated a reduction in leaf size accompanied by the presence of surface wrinkles on the leaves (Additional file 1: Fig. S7). To ascertain the impact of *PmLBD3* on plant hormone equilibrium, we conducted additional assessments of the concentrations of auxin, gibberellin, and BL in both empty vector (EV) and overexpressing (OE) transgenic plant leaves. The levels of BL and auxin in the overexpressing plants exhibited a considerable reduction, measuring 0.29 and 0.37 times greater than that in the control group, respectively. The concentration of gibberellin exhibited a substantial rise, reaching 1.69 times that of the control group (Fig. 6e). We detected and compared the expression levels of *ToDWF4* involved in BR biosynthesis between the plants of empty-vector and over-expression line tobacco. Results showed that expression levels of the *ToDWF4* in over-expression line were significantly higher than that in empty-vector tobacco (Additional file 1: Fig. S8c). All these results suggested that *PmLBD3* over-expression line is BR-deficiency. At the same time, the expression of *ToBAS1* gene was significantly increased, indicating that *PmLBD3* overexpression line can accelerate brassinolide metabolism, rather than inhibiting brassinolide biosynthesis (Additional file 1: Fig. S8a). These results showed that *PmLBD3* affected the hormone balance in plants, decreased the content of active brassinolide, regulated the growth and development of plants, and caused dwarfing of plants.

Cytological investigations revealed notable reductions in the dimensions of internode cells in OE plants characterised by lower cell lengths and widths. These cells exhibited a more compact arrangement, leading to an enhanced cell count inside the internodes. Consequently, these alterations contributed to the shortened length of internodes and augmented stem thickness (Fig. 6f, Additional file 1: Fig. S9a–c). According to the available study findings, the primary mechanism governing cell growth through the auxin pathway involves the induction of a SAUR protein by auxin [43]. To further elucidate the impact of the *PmLBD3* gene on plant cell expansion, this study examined the expression levels of *PmLBD3* in the transcriptome in relation to the significantly differentially expressed SAUR family genes (Additional file 1: Fig. S10). The findings revealed a significant negative correlation between the expression levels of the *PmLBD3* and *PmSAUR36a* genes, suggesting a potential interaction between the two. The results of Y1H and EMSA experiments showed that *PmLBD3* could bind to the *PmSAUR36a* promoter, and the double luciferase reporter gene assay results showed that *PmLBD3* inhibited *PmSAUR36a* expression. *PmSAUR36a* shared structural similarities with the AtSAUR36 protein found in Arabidopsis (Additional file 1: Fig. S11a). Previous studies in Arabidopsis have demonstrated that *AtSAUR36* inhibits cell enlargement [18]. Based on this knowledge, we hypothesised that *PmSAUR36a* may also influence cell size. To test this hypothesis, we transiently overexpressed *PmSAUR36a* in tobacco leaves and observed morphological changes in cell size under a microscope after 7 days. A total of 100 cell areas were measured. The cell area of tobacco leaves decreased following *PmSAUR36a* overexpression, supporting the notion that *PmSAUR36a* plays a role in regulating cell size (Additional file 1: Fig. S11b, c). In summary, *PmLBD3* downregulated *PmSAUR36a* expression and affected cell expansion by binding to the *PmSAUR36a* promoter region (Fig. 6g–i). However, *PmARF3* did not demonstrate a binding capability to the *PmSAUR36a* promoter (Additional file 1: Fig. S6b).

Discussion

The phenomenon of dwarfing resulting from the interaction between the rootstock and scion holds significant research implications in the fields of fruit tree breeding and production. The utilisation of dwarfing rootstocks has the potential to decrease cultivation density, improve productivity, and streamline cultivation procedures effectively [4]. Mume rootstock 'Lve', which was used in this study, showed a notable dwarfing ability compared to peach rootstock 'Zhongtaokangzhen No.1', effectively controlling the development of the scions. Compared with the control group, the scions were more significantly

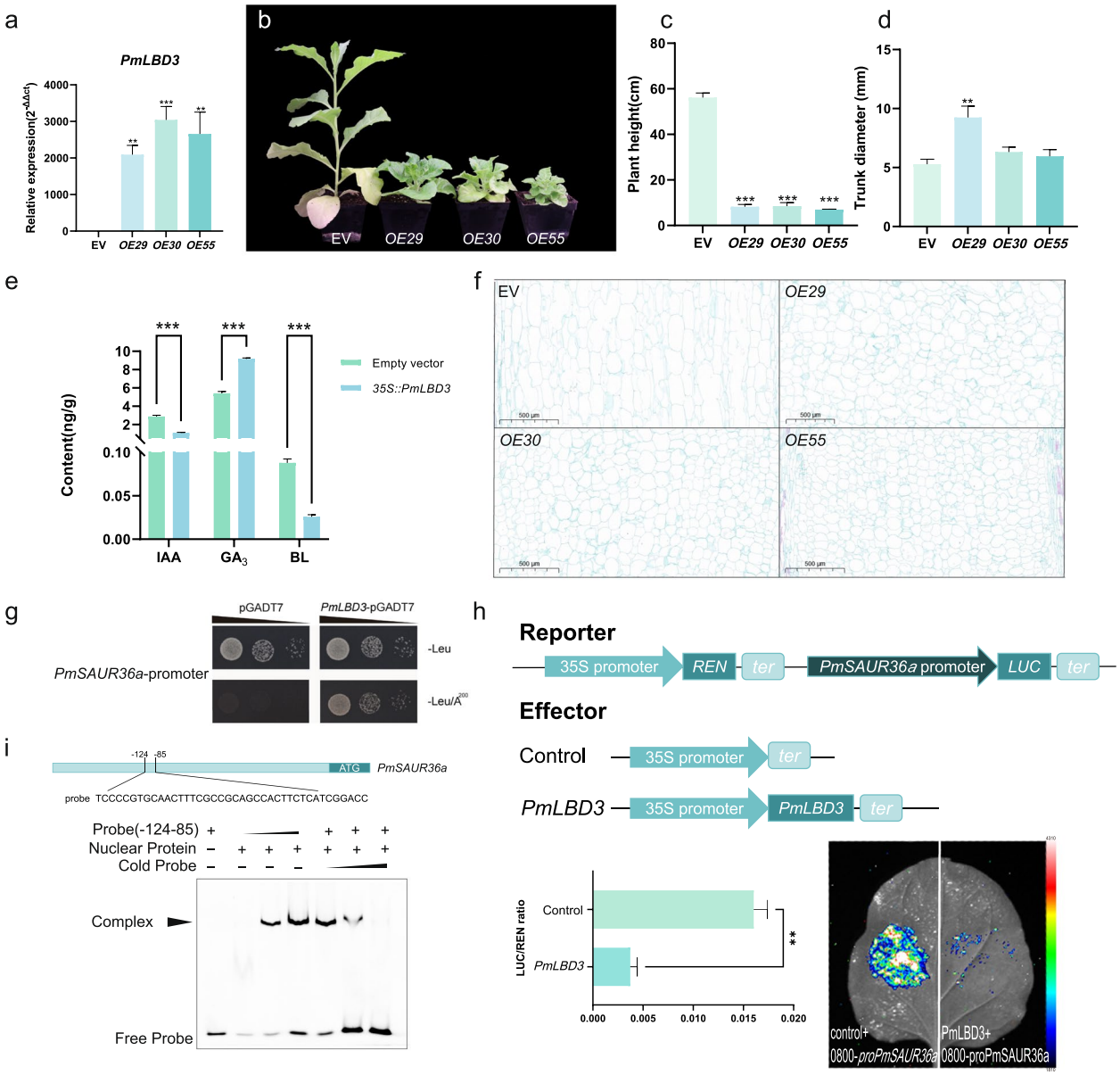

Fig. 6 *PmLBD3* overexpression reduces plant height and affects plant hormone balance and cell expansion. **a** Relative expression levels of *PmLBD3* in the empty vector (EV) and *PmLBD3*-overexpressing plants. Each result in the dataset represents the mean value together with its corresponding SE, which was calculated based on three biological replicates ($n=3$). The Student's test revealed that the presence of an asterisk denotes a statistically significant difference between the empty vector and transgenic lines (**$P<0.01$, ***$P<0.0001$). **b** Comparison of EV and *PmLBD3*-overexpressing tobacco phenotypes. Seven-centimetre scale bar. **c** Plant height of EV, *OE29*, *OE30*, and *OE55* ($n=5$). **d** Plant stem thickness for EV, *OE29*, *OE30*, and *OE55* ($n=5$). **e** The levels of endogenous IAA, GA_3, and BL content were measured in both EV and plants overexpressing the *PmLBD3* gene. In the range of conditions, the data presented in **c**–**e** reflects the mean value with the standard error ($n=3$). Student's *t*-test was employed to assess the statistical significance of differences between the EV and transgenic plants. Asterisks were used to denote significant differences (*$P<0.05$, **$P<0.01$, ***$P<0.0001$). **f** Longitudinal sections of stems in EV, *OE29*, *OE30*, and *OE55* plants. Scale bar = 500 μm. **g** Interactions of *PmLBD3* with the *PmSAUR36a* promoters detected in Y1H. -Leu stands for a culture medium without leucine, while -Leu.^{200} stands for a culture medium without leucine with 200 ng/mL of AbA. PGADT7 represents the negative control. **h** Double luciferase assay used to detect the regulation of *PmLBD3* on the *PmSAUR36a* promoter ($n=3$). **i** His-*PmLBD3* recombinant protein can bind specific DNA fragments in the *PmBAS1* promoter regions. Supporting data for individual data values in the figure legend are shown in Additional file 3

inhibited by growth, with a shorter scion length, shorter internode length, thinner cork layer cells in the stem, and a decrease in the number of cells near the xylem vessels (Fig. 1, Additional file 1: Fig. S1). This indicates that the mume rootstock is a good material for studying the mechanism of scion dwarfing.

To explore the precise mechanisms by which mume rootstocks regulate scion vigour, we conducted transcriptomic and metabolomic analyses of different tissue components in grafted plants grown on both mume and peach rootstocks. During transcriptional regulation, DEGs generated by the scion following grafting onto the mume rootstock were notably enriched in processes related to hormone response, auxin signalling, and flavonoid synthesis within the GO pathway. This enrichment included pathways, such as the auxin-activated signalling pathway, cellular response to auxin stimulus, transporter activity, naringenin-chalcone synthase activity, and flavonoid biosynthetic process (Fig. 3a). Similarly, KEGG enrichment analysis revealed a similar trend of enrichment, with significant enrichment observed in plant hormone signal transduction, BL biosynthesis, and flavonoid biosynthesis. The possible reason is that the control of scion vitality by mume rootstocks is mainly achieved by affecting hormone balance (Fig. 3b). Many research teams have also reported the regulatory effect of rootstocks on endogenous plant hormones in scions. Dwarfing rootstocks often affect the content of growth hormones in scions, thereby affecting the plant growth process [3, 6, 44]. Our hormone analysis results indicate that the BL content in the scion leaves and stems grafted on mume rootstocks was significantly reduced. The significant enrichment of auxin signalling pathway DEGs in the transcriptional analysis results suggests that mume rootstocks may affect the signal transduction of auxin in scions, thereby affecting the BL content. By comparing the DEGs in the stem and graft union of mume rootstock (LM-G/LM-S) with the DEGs in the stem and graft interface of peach rootstock (LP-G/LP-S), certain transcription factors were shown to be uniquely expressed in mume rootstock plants. This suggests that these transcription factors may be specifically controlled by the mume rootstock and play a crucial role in regulating scion dwarfing in the mume rootstock (Additional file 1: Fig. S12).

Previous studies have suggested that the polar transport of auxin is influenced by flavonoids and flavonol compounds, which interfere with plant development [45]. Multiple studies have consistently supported the notion that flavonoids function as endogenous negative regulators of auxin transport [45–49]. An investigation on peanut stems exhibiting varying plant heights revealed a notable drop in the concentrations of flavonoid metabolites, including L-epicatechin, quercetin, and naringin C-hexoside, in dwarf plants [50]. Similar research results have been validated in pears [51]. This discovery is consistent with the changes in metabolic substances in mume rootstock plants in this study. Our metabolomic analysis results showed that DAMs are significantly enriched in the flavonoid biosynthesis pathway (Fig. 4a). Furthermore, a notable reduction in flavonoid metabolites was observed in the mume rootstocks in comparison to the peach rootstocks (Additional file 1: Fig. S13). This change is also reflected in the binding site between the two rootstocks and scions, indicating that flavonoid metabolites may also play a role in the healing process of grafting wounds. Hence, it is speculated that the obvious decrease in metabolites within the flavonoid synthesis pathway in mume rootstocks, compared to peach rootstocks, could potentially impact the transportation and signalling of auxin between scions and rootstocks. This change may potentially affect the efficiency of auxin response and the expression levels of downstream transcription factors, thus regulating the plant growth process. Consequently, this imbalance in hormone levels may have repercussions on plant height. However, further investigation on the mechanisms via which mume rootstocks impede flavonoid production and their impacts on auxin transportation is required.

Plant hormones are widely involved in the regulation of plant growth and development. Many studies have documented that the manifestation of plant dwarfism can be attributed to the differential expression of genes involved in plant hormone metabolism and signal transmission [52–58]. The validation of the regulation of plant height by BL has been confirmed in various species, and the absence of genes associated with BL production or signal transduction can result in a reduction in plant height [59–61]. BAS1 is a key gene in the BL synthesis pathway and is mainly responsible for inactivating BL [27, 62]. The homologous gene of BAS1 has been shown to inactivate brassinolide in carrot [59], cotton [63], and tomato [64], so we hypothesised that *PmBAS1* also has a similar function. In this study, the expression level of *PmBAS1* was significantly upregulated (Fig. 3d), consistent with the decrease in BL content in mume rootstock plants (Fig. 1f). In previous studies, the *AtBAS1* gene was affected downstream of the LBD family transcription factor *AtLOB* [37]. Consistent with previous findings, the expression level of *PmLBD3* in the LBD gene family was significantly upregulated in mume rootstock plants (Additional file 2: Table S3), and direct binding to the *PmBAS1* promoter promoted its expression. This conclusion was supported by Y1H, dual luciferase detection, and EMSA experimental results (Fig. 5a–c). Meanwhile, there was a significant correlation between *PmLBD3*

and DAMs in different key metabolic pathways after transplantation, such as flavonoid biosynthesis and carbohydrate metabolism (Fig. 4b–d). Based on the above analysis results, we believe that *PmLBD3* may be a key gene affecting BL metabolism processes to control plant dwarfing. This hypothesis was supported by the observation of reduced plant height and shorter internodes in transgenic tobacco plants overexpressing *PmLBD3* (Fig. 6a–d). The hormone analysis findings of transgenic tobacco provide additional evidence to support the inhibitory impact of *PmLBD3* on BL (Fig. 6e). In transgenic *PmLBD3* plants, the expression of the homologous BAS1 gene in tobacco was significantly increased (Additional file 1: Fig. S8a), demonstrating the role of the BAS1 gene in inhibiting the BL content in overexpressing plants.

The impact of auxin on plant height has a high degree of complexity. The stunted growth observed in plants in the absence of auxin can be attributed to significant developmental impairments [65–67]. Additionally, several investigations have revealed that elevated amounts of auxin can hinder plant height [65, 68, 69]. There was an auxin-responsive AuxRE motif (TGTCTC) in the *PmLBD3* promoter. After experimental verification, the ARF family transcription factor PmARF3 was shown to bind to the *PmLBD3* promoter and upregulate its expression (Fig. 5d–f). Prior studies in *Arabidopsis* have suggested that LBD genes *AtLBD16*, *AtLBD17*, *AtLBD18*, and *AtLBD29* play a role downstream of *AtARF7* and *AtARF19* in auxin signalling transduction, mainly regulating lateral root formation, callus induction, or adventitious root formation [39, 60, 70–72]. However, in this study, *PmLBD3* further regulated the expression of *PmBAS1* after being influenced by auxin signalling, affecting the inactivation process of BL and forming a joint regulatory network of ARF-LBD-BAS1. Research in apples has found that *MdARF3* is located at the main site of rootstock-induced dwarfing, which may have a potential role in dwarfing rootstocks [73]. This finding supports our conjecture that *PmLBD3* is involved in the process of plant dwarfing and that *PmLBD3* may be a downstream gene involved in the role of ARF3 in dwarfing rootstocks, linking growth hormone and oleoresin lactone content in the regulation of plant height in plants. Consequently, these molecular interactions have a profound influence on the growth and development of plants. Interestingly, a notable reduction in BL and IAA levels was seen in tobacco plants overexpressing *PmLBD3*. Conversely, the GA_3 content increased (Fig. 6e). Given the deficiency of IAA and BL content in the plant, it is hypothesised that an increase in GA_3 content is necessary for the plant to maintain normal physiological functions. This process may involve a feedback mechanism within the phytohormone network. This indicates that there is still an unknown regulatory relationship between *PmLBD3* and the balance of growth hormones in plants.

In contrast, earlier research has postulated a correlation between the dwarfing process of plants and alterations in stem elongation and associated cellular mechanisms [12, 74]. In this study, scions on mume rootstocks exhibited smaller cell volumes and thinner phloem compared to peach rootstocks (Additional file 1: Fig. S1). This change may be related to DEGs regulating cellular processes. SAURs are one of the main effector factors of auxin-mediated cell expansion, which can promote cell expansion. Studies have suggested that some SAURs negatively regulate cell expansion [18, 75–77], but the mechanism of action is not yet clear. In the transcriptome, we found a significant negative correlation between *PmSAUR36a* and *PmLBD3* expression (Additional file 1: Fig. S10). It is postulated that a potential regulatory link exists between these two genes. The subsequent experimental results confirmed this hypothesis, as *PmLBD3* bound to the *PmSAUR36a* promoter and inhibited its expression in plants (Fig. 6g–i). Transient overexpression of *PmSAUR36a* in tobacco leaves affected the cell area of the tobacco leaves (Additional file 1: Fig. S11b, c). The suppression of *PmSAUR36a* expression by *PmLBD3* also explained why stem cell size was altered in tobacco plants overexpressing *PmLBD3* (Fig. 6f, Additional file 1: Figs. S8b and S9a–c). In addition, after exogenous IAA treatment of mume leaves, we detected that the expression levels of the *PmARF3* and *PmLBD3* genes were significantly upregulated, while the expression levels of *PmSAUR36a* were significantly downregulated (Additional file 1: Fig. S11d), which was consistent with the previous experimental results. These results suggest that *PmLBD3* is involved in the auxin signalling pathway by inhibiting *PmSAUR36a* and affecting cell size.

Conclusions

The research findings reported in this study elucidate the participation of *PmLBD3* in the complex hormonal network of auxin signalling that regulates the BL metabolism pathway (Fig. 7). The involvement of *PmLBD3* in the auxin signalling pathway occurred in a downstream capacity, with its regulation directly influenced by *PmARF3*. Overexpression of this gene enhanced BL metabolism, resulting in a decrease in endogenous BL levels. This alteration in brassinolide levels has significant effects on cell size and morphology. At the same time, PmLBD3 interferes with the normal regulatory mechanism of cell expansion by inhibiting the expression of *PmSAUR36a*. *PmLBD3* overexpression promotes rapid cell division and proliferation, but also leads to a reduction in the size of each cell due to rapid division. Furthermore, *PmLBD3* upregulation led to an increase in GA_3

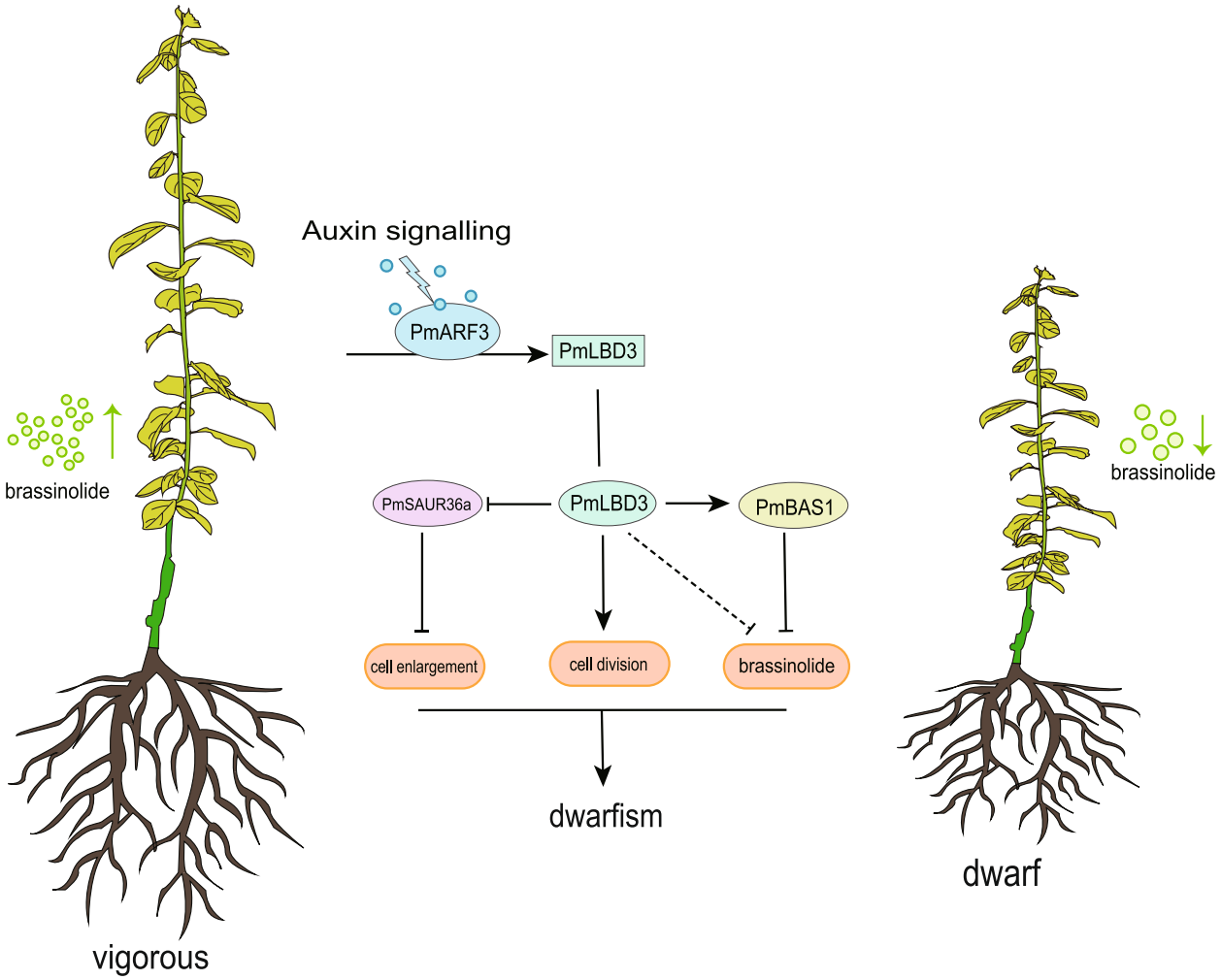

Fig. 7 *PmLBD3*, a key transcription factor, coordinates hormone balance through the auxin and brassinolide pathways, leading to the molecular mechanism of mume dwarfism. The direct interaction is represented by a solid line, while the indirect effect is represented by a dashed line

production and a decrease in IAA production. This suggests the existence of a feedback regulatory mechanism involving IAA in the control of *PmLBD3*. Additional investigation into the regulatory mechanisms governing hormone networks in plants is necessary. The research conducted significantly enhanced our comprehension of the regulatory network that exists between auxin and BL. Specifically, it has provided insights into the molecular mechanism through which *PmLBD3*, a crucial transcription factor, orchestrates the equilibrium of hormones by interacting with the auxin and BL pathways. Consequently, this coordination ultimately results in the manifestation of mume dwarfism.

Methods

Plant materials and growth conditions

This study was performed at the National Field Genebank for *Prunus mume* and Waxberry at Nanjing Agricultural University in China from March to September 2022 and 2023. As test material, commercial mume scion 'Longyan (L)', peach scion 'Hujingmilu (H)', and mume (M) rootstock 'Lve (LVE)' and peach (P) rootstocks 'Zhongtaokangzhen No.1 (ZTKZ)' were used. 'Longyan' was grafted onto mume (LM), and 'Longyan' was grafted onto peach (LP). The mume rootstock 'Lve' was obtained from the commercial production of 1-year cuttings purchased from Xinyi Green Golden Flower and Wood Professional Cooperative (Xuzhou, China). The peach rootstock 'Zhongtaokangzhen No.1' was obtained from the Zhengzhou Institute of Fruit Trees, Chinese Academy of Agricultural Sciences (Zhengzhou, China), as an annual cutting seedling.

The rootstock was planted in a 25-cm diameter plastic basin and grown in a substrate mixture of peat, sand, and soil in a 1:1:3 (v:v:v) ratio. The plants were nurtured in a standard greenhouse environment for 3 months prior to

grafting, with the rootstock being pruned to a height of 30 cm above ground level. In January, scions from 'Longyan' and 'Hujingmilu' trees were taken and grafted at a height of 30 cm onto 1-year-old mume and peach rootstocks. On the 125th day post-grafting, 6 plants were randomly chosen from the LM and LP combinations. The leaves, stems, grafting interfaces, and roots were then frozen in liquid nitrogen for metabolome analysis samples, with three of them also being used for transcriptome analysis. After the samples were collected, they were kept at − 80 °C until they were used in other studies.

Hormone treatments

At 75 days after grafting, peach rootstock and mume rootstock plants were sprayed with water or BL (0.5 mg/L) and treated every 10 days. Following a series of six successive treatments, the lengths of the newly emerged plant shoots were quantified, and leaf samples were collected for further analysis. Following the quick freezing process using liquid nitrogen, the plants were then stored at − 80 °C in preparation for future experimental procedures. Mume rootstock plant leaves were treated with a solution containing 50 mg/L IAA, 50 mg/L GA_3, and 0.5 mg/L BL. Samples were collected 24 h after treatment for quantitative real-time polymerase chain reaction (qRT-PCR). IAA (B21810), GA_3 (B20187), and BL (B21633) hormone standards from Shanghai yuanye Bio-Technology Co., Ltd. (Shanghai, China).

Phenotypic analysis

After 75 days after grafting, the primary shoot length (cm), number of nodes, and intermediate length (mm) of two grafting combinations were measured every 10 days. Vernier callipers were used to measure scion diameter. Internode slices from peach and mume scion plants were fixed using formalin-aceto-alcohol (FAA) solution. The sample was dehydrated in an ethanol gradient, stained with safranine solid green, and photographed at the longitudinal section of the internodes under a microscope.

RNA extraction and library preparation

The isolation of total RNA was carried out using the Foregene Nuclear Acid Extraction Kit (Shenzhen, China), followed by purification using RNase-free DNase I as per the instructions provided by the manufacturer (TaKaRa, Japan). Additionally, gel electrophoresis was utilised to evaluate the quality of the RNA samples. Following that, the RNA underwent treatment with oligo (dT) and was combined with fragment buffer to facilitate the synthesis of the first-strand cDNA. Following the purification process, the fragment underwent purification using single-nucleotide addition and EB end repair. The linking products were amplified using polymerase chain reaction (PCR) technology, and sequencing was performed using the Illumina HiSeq 4000 platform (BGI, Beijing, China).

Analysis of transcriptome sequencing

Following the sequencing process, the quality of the initial reads was assessed using FastQC (version 0.11.9). Subsequently, the command line employed SOAPnuke (version 1.4.0) software to remove reads of inferior quality, adaptor sequences, and bases of unknown origin. We employed HISAT version 2.1.0 to align high-quality sequencing reads against the *P. mume* reference genome, accessed from the National Center for Biotechnology Information (NCBI) website (https://www.ncbi.nlm.nih.gov/genome/?term=prunus%20mume) [78]. The gene expression levels were calculated using RSEM version 1.2.8, and the expression values were reported in fragments per kilobase of transcript per million mapped reads (FPKM) [79]. The DESeq R software tool was employed [80] to detect DEGs across several datasets.

Gene ontology and KEGG pathway analysis

The phyper package in R software was utilised to conduct an enrichment study on graphene oxide. The genes under investigation were categorised into three distinct groups: molecular function, biological processes, and cellular components [81]. GO analysis is a common method used to assess the functional enrichment of DEGs. In this analysis, a false discovery rate (FDR) threshold of less than or equal to 0.05 was considered statistically significant enrichment of DEGs. Additionally, enrichment pathways were obtained by conducting KEGG pathway analysis.

Metabolome profiling

Following a grafting period of 125 days, samples were collected from several plant components, including the roots, stems, leaves, and grafting interfaces. Six biological replicates were collected from each location for the purpose of isolating and detecting metabolites. The Waters 2777C UPLC (Waters, Milford, USA) was employed in conjunction with the Q Active HF high-resolution mass spectrometry (Thermo Fisher Scientific, MA, USA) for this analysis. The offline data obtained from mass spectrometry were imported into Compound Discoverer 3.2 software, developed by Thermo Fisher Scientific (USA). This programme was utilised in conjunction with the BMDB (BGI Metabolome Database), mzCloud database, and ChemSpider online database to conduct a comprehensive analysis of the mass spectrometry data.

This study analysed the functions of the pathways using the KEGGPATHWAY database to identify the primary biochemical metabolic and signal transduction pathways associated with metabolites. The variable importance in projection (VIP) of variables was computed to assess

the magnitude of influence and explanatory capacity of individual metabolite expression patterns on the classification and discrimination of sample groups. This aided in the identification of metabolic markers during the screening process. A sevenfold cross-validation technique was used during the model construction process. The methodology known as OPLS-DA is a fusion of the orthogonal signal correction (OSC) and partial least squares discriminant analysis (PLS-DA) techniques. By eliminating the information that is irrelevant to classification, this approach effectively reduces the model's complexity and enhances its explanatory capacity while preserving its predictive accuracy.

Quantitative analysis of endogenous hormones in plants

To measure the changes in endogenous hormone content in grafted plant leaves, on the 125th day after grafting, complete leaves from three directions in the middle of each scion of the plant were collected and frozen with liquid nitrogen. Every two plant samples from the same grafting combination were mixed in liquid nitrogen and ground into powder. They were considered one biological replicate, and three independent biological replicates were conducted. BL was extracted at 4 °C with 80% methanol and 20% water, and subsequent extraction methods followed Zhao and Huo [82]. IAA and GA_3 were extracted from transgenic and blank tobacco leaf samples in isopropanol at 4 °C.

A quantitative investigation was conducted on endogenous hormones using LC–MS/MS with the Agilent 1290 high-performance liquid chromatography system (Agilent, Santa Clara, CA, USA) and the AB Scienx QTRAP 6500 tandem mass spectrometry instrument (Applied Biosystems, Foster City, CA, USA).

Transformation and characterisation of transgenic plants

To create transgenic plants with enhanced *PmLBD3* expression, PCR amplified the entire coding region using the primers listed in Additional file 2: Table S4. We next introduced the amplified sequence into the CaMV35S-promoted pCambia1301 vector. The vector was translocated into *Agrobacterium tumefaciens* EHA105 and transmitted to tobacco plants via leaf discs. After transgenic plant T1 generation and empty vector plant maturity, the morphological characteristics were examined. Paraffin sections of transgenic tobacco stem tissues were observed afterwards. The cell count was determined by quantifying the number of cells inside a given area while concurrently utilising ImageJ software to measure the length and width of the cells. Measurements were recorded on a minimum of 100 cells within each longitudinal section of the stem.

Transient overexpression assays

Three-week-old tobacco plants were employed for transient overexpression. To create the overexpression constructs, the full-length CDSs of *PmSAUR36a* were amplified by PCR and inserted into the pCambia1301 vector. The recombinant plasmids or empty vectors were transformed into *Agrobacterium tumefaciens* EHA105 cells, subsequently resuspended in infiltration buffer (10 mm MES, 10 mm MgCl2, 100 mm acetosyringone, pH 5.7), and allowed to grow to an OD600 of 0.6. After incubation at room temperature for 2–3 h, they were injected into tobacco leaves and cultured for 7 days. Three independent lines were generated for both *PmSAUR36a*. To ensure the reliability of the experimental results, we injected the treatment group and the empty vector on the left and right ends of the same leaf, and each leaf was used as a biological replicate. At the end of the experiment, the leaves were collected for microscopic observation.

RNA extraction and quantitative real-time polymerase chain reaction

The samples were subjected to RNA extraction using the Trelief® RNAprep Pure Plant Plus Kit (TSINGKE, Beijing China). Subsequently, the extracted RNA was reverse transcribed into cDNA using the PrimeScript™ RT reagent kit from Takara (Kusatsu, Japan). SYBR Green Pro TaqHS Premium (ACCURATE BIOLOGY, Hunan China) was used for the qRT-PCR reaction. The fluorescence quantitative PCR instrument employed in this study was QuantStudio 5 Flex (Applied Biosystems, MA, USA). The internal references utilised in this study were the *RPII* and *TUB8* genes. The analysis of relative expression levels was conducted using the $2^{-\Delta\Delta Ct}$ methodology. The qRT-PCR experiment involved the analysis of three independent biological replicates. The primer sequences employed for qRT-PCR are listed in Additional file 2: Table S4.

Yeast one-hybrid assay

PmLBD3-pGADT7 and *PmARF3*-pGADT7 prey vectors were created by amplifying and cloning their cDNA into the pGADT7 vector. Amplification of DNA segments containing the predicted binding sites in *PmBAS1*, *PmSAUR36a*, and *PmLBD3* promoters was done using primers developed for this purpose (Additional file 2: Table S4). The amplified promoter was combined with pAbAi to create bait vectors pAbAi-*PmBAS1*, pAbAi-*PmSAUR36a*, and pAbAi-*PmLBD3*. Nutrient-deficient SD-Ura medium was inoculated with bait vector-derived yeast strain Y1H Gold. Following this, the prey vector was introduced into yeast strain Y1H Gold harbouring the bait vector and cultivated on SD-Leu medium. The

diluted solution was placed on SD-Leu medium with or without AbA (aureobasidin A) after diluting the yeast culture containing positive clones with SD-Leu liquid media to an OD600 of 0.2.

Dual-luciferase transcriptional activity assay

The 2000-bp promoter regions of *PmLBD3*, *PmBAS1*, and *PmSAUR36a* were inserted into the pGREENII 0800-LUC reporting vector. We employed pCambia1301-*PmLBD3* and pCambia1301-*PmARF3* as effector vectors, while pCambia1301 served as the control. All vectors were transferred into *Agrobacterium tumefaciens* GV3101 (pSoup) competent cells. The experimental procedure involved the combination of *Agrobacterium* cells harbouring both reporting and effector components at a ratio of 9:1. Transient expression in *Nicotiana benthamiana* was performed according to the method described by Hellens [83]. The Dual-Luciferase Reporter Assay System (Promega, WI, USA) was employed to detect luciferase activity, and an Infinite200 Pro microplate reader (Tecan, Männedorf, Switzerland) was used for the measurements. Expression was quantified by calculating the ratio of LUC to REN activity and then normalising it to the negative control infiltration.

Electrophoretic Mobility Shift Assay (EMSA)

The pCold-*PmLBD3* recombinant protein lacking a termination codon was produced and purified with the addition of a histidine tag for the purpose of conducting an EMSA. We also synthesised 40-bp 5′ Fam-labelled probes that covered the predicted binding areas of the *PmBAS1* and *PmSAUR36a* promoters. In this experimental setup, comparable DNA fragments lacking any specific labelling (referred to as 'cold probes') were employed as competitive agents. The EMSA binding process was performed in accordance with the guidelines provided by the manufacturer (Chemiluminescent EMSA Kit; Beyotime, Shanghai, China). An ample surplus of competitor DNA, specifically of a cold nature, was incorporated at a minimum of a 20-fold excess compared to the quantity of the labelled probe. The protein–DNA complex was resolved using a 6% polyacrylamide gel [84]. The Tanon5200 chemiluminescence imaging system was used for SDS-PAGE imaging, while the ChemiDocTMXRS + system (Bio Rad, CA, USA) was used for scanning.

Data analysis

GraphPad Prism7.0, SPSS 20, and Excel were used to analyse the experimental data, and PS and AI were used for image processing. The gene names used in the paper correspond to the gene IDs provided in Additional file 2: Table S5.

Abbreviations

IAA	Indole-3-acetic acid
SAUR	Small auxin-up RNA
BRs	Brassinosteroids
LBDs	Lateral organ boundaries domains
LOB	The lateral organ boundaries
GUS	β-Glucuronidase
ARF	Auxin response factor
DEGs	Differentially expressed genes
GA_3	Gibberellic acid
BL	Brassinolide
ZTKZ	Zhongtaokangzhen No.1
LVE	Lve
LP	'Longyan/Peach'
LM	'Longyan/Mume'
L	Leaves
S	Stems
G	Grafting interfaces
R	Roots
SE	Standard error
qRT-PCR	Quantitative real-time polymerase chain reaction
LC–MS/MS	Liquid chromatography-tandem mass spectrometry
OPLS-DA	Orthogonal partial least squares discriminant analysis
DAMs	Differential accumulated metabolites
GO	Gene Ontology
KEGG	Kyoto Encyclopedia of Genes and Genomes
Y1H	Yeast one-hybrid
EMSA	Electrophoretic mobility shift assay
DNA	Deoxyribonucleic acid
EV	Empty vector
OE	Overexpressing
FAA	Formalin-aceto-alcohol
FPKM	Fragments per kilobase of transcript per million mapped reads
FDR	False discovery rate
VIP	Variable importance in projection
OSC	The orthogonal signal correction
PLS-DA	Partial least squares discriminant analysis

Supplementary Information

The online version contains supplementary material available at https://doi.org/10.1186/s12915-024-01985-z.

Additional file 1: Fig. S1 'Hujingmilu' grafted on P. mume and P. persica rootstocks demonstrates distinct growth discrepancy. And the shape of stem cells is different in P. mume and P. persica rootstocks that have been grafted. Fig. S2 Hormone content in tissues of different rootstock and scion combinations. Fig. S3 Validation of RNA-Seq data by real-time quantitative qRT-PCR. Fig. S4 OPLS-DA analysis of metabolites after grafting with different rootstock combinations. Fig. S5 Analysis of PmLBD3 gene. Fig. S6 Y1H validation of ARF transcription factor regulation relationship. Fig. S7 Significant differences in overexpression of PmLBD3 in transgenic tobacco leaves. Fig. S8 The gene expression of overexpressed PmLBD3 tobacco was detected by real-time quantitative qRT-PCR. Fig. S9 Morphological statistics of transgenic tobacco stem paraffin sections. Fig. S10 Analysis of the relationship between the way of PmLBD3 gene is expressed and the genes from SAUR gene family. Fig. S11 PmSAUR36a affects cell size. Fig. S12 Analysis of differential expression of transcription factor Venn in different tissues. Fig. S13 Metabolic heat map of flavonoids in different rootstock and scion combinations

Additional file 2: Table S1 The expression level of BAS1 gene in transcriptome. Table S2 Different rootstock ear combinations' differentially accumulated metabolites' KEGG enrichment analysis. Table S3 Expression levels of differentially expressed genes in the LBD family in the transcriptome. Table S4 Primers used in this study. Table S5 The gene name used in this paper corresponds to the gene ID

Additional file 3: Supporting data for individual data values in the figure legend

Additional file 4: Uncropped gels/blots for Fig. 5a, Fig. 5c, Fig. 5e, Fig. 6g, Fig. 6i, and Fig. S6

Acknowledgements
We would like to thank the National Field Genebank for *Prunus mume* and Waxberry at Nanjing Agricultural University in China for providing plant materials and site facilities.

Authors' contributions
Y.M. and Z.G. conceived the project. Y.M. and C.M. performed most of the experiments and data analysis. P.Z. provided technical support for transgenic experiments. Y.M. performed the transcriptome analysis under the supervision of W.T. and H.X. F.G., Y.B., M.L., Z.W., and F.H. assisted with experiments and data analysis. Z.N. assists in the management and care of plant materials. Y.M. wrote the manuscript. C.M., T.S., and Z.G. revised the manuscript. All authors approved the manuscript.

Funding
This work was supported by the National Natural Science Foundation of China (32372670, 31971703), the Jiangsu Agricultural Industry Technology System (JATS [2023]432), and the Priority Academic Program Development of Jiangsu Higher Education Institutions (PAPD).

Availability of data and materials
All data generated or analysed during this study are included in this published article, its supplementary information files, and publicly available repositories. The clean data for the DEG analysis were deposited in the NCBI SRA (PRJNA1055178) [85]. All untargeted metabolomic data used in this publication were deposited in the EMBL-EBI MetaboLights database under identifiers MTBLS10051 [86], MTBLS10062 [87], and MTBLS10083 [88]. Supporting data for individual data values in the figure legend are shown in Additional file 3.

Declarations

Ethics approval and consent to participate
Not applicable.

Consent for publication
Not applicable.

Competing interests
The authors declare that they have no conflicts of interest.

Received: 12 March 2024 Accepted: 15 August 2024
Published online: 26 August 2024

References

1. Luo J, Tang Y, Chu Z, Peng Y, Chen J, Yu H, et al. SlZF3 regulates tomato plant height by directly repressing SlGA20ox4 in the gibberellic acid biosynthesis pathway. Hortic Res. 2023;10:uhad025.
2. Hayat F, Ma C, Iqbal S, Ma Y, Khanum F, Tariq R, et al. Comprehensive transcriptome profiling and hormonal signaling reveals important mechanism related to dwarfing effect of rootstocks on scion in Japanese apricot (*Prunus mume*). Sci Hortic. 2023;321:112267.
3. Cong L, Ling H, Liu S, Wang A, Zhai R, Yang C, et al. 'Yunnan' quince rootstock promoted flower bud formation of 'Abbé Fetel' pear by altering hormone levels and PbAGL9 expression. J Plant Physiol. 2023;282:153924.
4. Gu Q, Wei Q, Hu Y, Chen M, Chen Z, Zheng S, et al. Physiological and full-length transcriptome analyses reveal the dwarfing regulation in trifoliate orange (*Poncirus trifoliata* L.). Plants. 2023;12:271.
5. Hayat F, Li J, Iqbal S, Khan U, Ali NA, Peng Y, et al. Hormonal interactions underlying rootstock-induced vigor control in horticultural crops. Appl Sci. 2023;13:1237.
6. Li X, Wang Y, Zhao L, Chen S, Yuan Y, Wei T, et al. Effects of *Cerasus humilis (Bge). Sok.* Rootstock on peach growth, development, and expression of growth-related genes. Horticulturae. 2023;9:576.
7. Foster TM, Celton J-M, Chagné D, Tustin DS, Gardiner SE. Two quantitative trait loci, Dw1 and Dw2, are primarily responsible for rootstock-induced dwarfing in apple. Hortic Res. 2015;2:15001.
8. Prassinos C, Ko J-H, Lang G, Iezzoni AF, Han K-H. Rootstock-induced dwarfing in cherries is caused by differential cessation of terminal meristem growth and is triggered by rootstock-specific gene regulation. Tree Physiol. 2009;29:927–36.
9. Zhou Y, Underhill SJR. Differential transcription pathways associated with rootstock-induced dwarfing in breadfruit (*Artocarpus altilis*) scions. BMC Plant Biol. 2021;21:261.
10. Tworkoski T, Fazio G. Hormone and growth interactions of scions and size-controlling rootstocks of young apple trees. Plant Growth Regul. 2016;78:105–19.
11. Aloni B, Cohen R, Karni L, Aktas H, Edelstein M. Hormonal signaling in rootstock–scion interactions. Sci Hortic. 2010;127:119–26.
12. Yang S, Zhang K, Zhu H, Zhang X, Yan W, Xu N, et al. Melon short internode (CmSi) encodes an ERECTA-like receptor kinase regulating stem elongation through auxin signaling. Hortic Res. 2020;7:202.
13. Michalczuk L. Indole-3-acetic acid level in wood, bark and cambial sap of apple rootstocks differing in growth vigour. Acta Physiol Plant. 2002;24:131–6.
14. Song C, Zhang D, Zhang J, Zheng L, Zhao C, Ma J, et al. Expression analysis of key auxin synthesis, transport, and metabolism genes in different young dwarfing apple trees. Acta Physiol Plant. 2016;38:43.
15. Zhang S, Wang S, Xu Y, Yu C, Shen C, Qian Q, et al. The auxin response factor, OsARF19, controls rice leaf angles through positively regulating OsGH3-5 and OsBRI1. Plant Cell Environ. 2015;38:638–54.
16. Stortenbeker N, Bemer M. The SAUR gene family: the plant's toolbox for adaptation of growth and development. J Exp Bot. 2019;70:17–27.
17. Chae K, Isaacs CG, Reeves PH, Maloney GS, Muday GK, Nagpal P, et al. *Arabidopsis* SMALL AUXIN UP RNA63 promotes hypocotyl and stamen filament elongation. Plant J. 2012;71:684–97.
18. Hou K, Wu W, Gan S-S. *SAUR36*, a SMALL AUXIN UP RNA gene, is involved in the promotion of leaf senescence in *Arabidopsis*. Plant Physiol. 2013;161:1002–9.
19. Koka CV, Cerny RE, Gardner RG, Noguchi T, Fujioka S, Takatsuto S, et al. A putative role for the tomato genes DUMPY and CURL-3 in brassinosteroid biosynthesis and response. Plant Physiol. 2000;122:85–98.
20. Spartz AK, Lee SH, Wenger JP, Gonzalez N, Itoh H, Inzé D, et al. The SAUR19 subfamily of SMALL AUXIN UP RNA genes promote cell expansion. Plant J. 2012;70:978–90.
21. Stamm P, Kumar PP. Auxin and gibberellin responsive Arabidopsis SMALL AUXIN UP RNA36 regulates hypocotyl elongation in the light. Plant Cell Rep. 2013;32:759–69.
22. van Mourik H, van Dijk ADJ, Stortenbeker N, Angenent GC, Bemer M. Divergent regulation of *Arabidopsis* SAUR genes: a focus on the SAUR10-clade. BMC Plant Biol. 2017;17:245.
23. Fridman Y, Savaldi-Goldstein S. Brassinosteroids in growth control: how, when and where. Plant Sci. 2013;209:24–31.
24. Unterholzner SJ, Rozhon W, Papacek M, Ciomas J, Lange T, Kugler KG, et al. Brassinosteroids are master regulators of gibberellin biosynthesis in *Arabidopsis*. Plant Cell. 2015;27:2261–72.
25. Kim T-W, Guan S, Sun Y, Deng Z, Tang W, Shang J-X, et al. Brassinosteroid signal transduction from cell-surface receptor kinases to nuclear transcription factors. Nat Cell Biol. 2009;11:1254–60.
26. Jager CE, Symons GM, Nomura T, Yamada Y, Smith JJ, Yamaguchi S, et al. Characterization of two brassinosteroid C-6 oxidase genes in pea. Plant Physiol. 2007;143:1894–904.
27. Turk EM, Fujioka S, Seto H, Shimada Y, Takatsuto S, Yoshida S, et al. BAS1 and SOB7 act redundantly to modulate *Arabidopsis* photomorphogenesis via unique brassinosteroid inactivation mechanisms. Plant J. 2005;42:23–34.
28. Yang B, Zhou S, Ou L, Liu F, Yang L, Zheng J, et al. A novel single-base mutation in CaBRI1 confers dwarf phenotype and brassinosteroid accumulation in pepper. Mol Genet Genomics. 2020;295:343–56.
29. Yang M, Wang X. Multiple ways of BES1/BZR1 degradation to decode distinct developmental and environmental cues in plants. Mol Plant. 2017;10:915–7.

30. He G, Liu J, Dong H, Sun J. The blue-light receptor CRY1 interacts with BZR1 and BIN2 to modulate the phosphorylation and nuclear function of BZR1 in repressing BR signaling in *Arabidopsis*. Mol Plant. 2019;12:689–703.
31. Tong H, Xiao Y, Liu D, Gao S, Liu L, Yin Y, et al. Brassinosteroid regulates cell elongation by modulating gibberellin metabolism in rice. Plant Cell. 2014;26:4376–93.
32. Gallego-Bartolomé J, Minguet EG, Grau-Enguix F, Abbas M, Locascio A, Thomas SG, et al. Molecular mechanism for the interaction between gibberellin and brassinosteroid signaling pathways in *Arabidopsis*. Proc Natl Acad Sci U S A. 2012;109:13446–51.
33. Zhang Y, Li Z, Ma B, Hou Q, Wan X. Phylogeny and functions of LOB domain proteins in plants. Int J Mol Sci. 2020;21:E2278.
34. Sun X, Feng Z, Meng L, Zhu J, Geitmann A. *Arabidopsis* ASL11/LBD15 is involved in shoot apical meristem development and regulates WUS expression. Planta. 2013;237:1367–78.
35. Zentella R, Zhang Z-L, Park M, Thomas SG, Endo A, Murase K, et al. Global analysis of della direct targets in early gibberellin signaling in *Arabidopsis*. Plant Cell. 2007;19:3037–57.
36. Ikezaki M, Kojima M, Sakakibara H, Kojima S, Ueno Y, Machida C, et al. Genetic networks regulated by ASYMMETRIC LEAVES1 (AS1) and AS2 in leaf development in *Arabidopsis thaliana*: KNOX genes control five morphological events. Plant J. 2010;61:70–82.
37. Bell EM, Lin W, Husbands AY, Yu L, Jaganatha V, Jablonska B, et al. *Arabidopsis* lateral organ boundaries negatively regulates brassinosteroid accumulation to limit growth in organ boundaries. Proc Natl Acad Sci U S A. 2012;109:21146–51.
38. Jeon E, Young Kang N, Cho C, Joon Seo P, Chung Suh M, Kim J. LBD14/ASL17 positively regulates lateral root formation and is involved in ABA response for root architecture in *Arabidopsis*. Plant Cell Physiol. 2017;58:2190–201.
39. Pandey SK, Lee HW, Kim M-J, Cho C, Oh E, Kim J. LBD18 uses a dual mode of a positive feedback loop to regulate ARF expression and transcriptional activity in *Arabidopsis*. Plant J. 2018;95:233–51.
40. Teng R-M, Yang N, Liu C-F, Chen Y, Wang Y-X, Zhuang J. CsLBD37, a LBD/ASL transcription factor, affects nitrate response and flowering of tea plant. Sci Hortic. 2022;306:111457.
41. Feng X, Xiong J, Zhang W, Guan H, Zheng D, Xiong H, et al. ZmLBD5, a class-II LBD gene, negatively regulates drought tolerance by impairing abscisic acid synthesis. Plant J. 2022;112:1364–76.
42. Basile B, DeJong TM. Control of fruit tree vigor induced by dwarfing rootstocks. In: Warrington I, editor. Horticultural reviews. 1st ed. Wiley; 2018. p. 39–97.
43. Du M, Spalding EP, Gray WM. Rapid auxin-mediated cell expansion. Annu Rev Plant Biol. 2020;71:379–402.
44. Hayat F, Iqbal S, Coulibaly D, Razzaq MK, Nawaz MA, Jiang W, et al. An insight into dwarfing mechanism: contribution of scion-rootstock interactions toward fruit crop improvement. Fruit Res. 2021;1:1–11.
45. Kuhn BM, Geisler M, Bigler L, Ringli C. Flavonols accumulate asymmetrically and affect auxin transport in *Arabidopsis*. Plant Physiol. 2011;156:585–95.
46. Brown DE, Rashotte AM, Murphy AS, Normanly J, Tague BW, Peer WA, et al. Flavonoids act as negative regulators of auxin transport in vivo in *Arabidopsis*. Plant Physiol. 2001;126:524–35.
47. Kurepa J, Shull TE, Smalle JA. Friends in arms: flavonoids and the auxin/cytokinin balance in terrestrialization. Plants. 2023;12:517.
48. Peer WA, Murphy AS. Flavonoids and auxin transport: modulators or regulators? Trends Plant Sci. 2007;12:556–63.
49. Zhao X, Sun X-F, Zhao L-L, Huang L-J, Wang P-C. Morphological, transcriptomic and metabolomic analyses of *Sophora davidii* mutants for plant height. BMC Plant Biol. 2022;22:144.
50. Zang X, Liu J, Zhao J, Liu J, Ren J, Li L, et al. Uncovering mechanisms governing stem growth in peanut (*Arachis hypogaea* L.) with varying plant heights through integrated transcriptome and metabolomics analyses. J Plant Physiol. 2023;287:154052.
51. Cui Z, Zhang H, Galarneau E-RA, Yang Y, Li D, Song J, et al. Metabolome analysis reveals important compounds related to dwarfing effect of interstock on scion in pear. Ann Appl Biol. 2021;179:108–22.
52. Zou T, Zhang K, Zhang J, Liu S, Liang J, Liu J, et al. DWARF AND LOW-TILLERING 2 functions in brassinosteroid signaling and controls plant architecture and grain size in rice. Plant J. 2023;116:1766–83.
53. Zang X, Liu J, Zhao J, Liu J, Ren J, Li L, et al. Uncovering mechanisms governing stem growth in peanut (*Arachis hypogaea* L.) with varying plant heights through integrated transcriptome and metabolomics analyses. J Plant Physiol. 2023;287:154052.
54. Xie Z, Zhang L, Zhang Q, Lu Y, Dong C, Li D, et al. A Glu209Lys substitution in DRG1/TaACT7, which disturbs F-actin organization, reduces plant height and grain length in bread wheat. New Phytol. 2023;240:1913–29.
55. El-Kereamy A, Bi Y-M, Mahmood K, Ranathunge K, Yaish MW, Nambara E, et al. Overexpression of the CC-type glutaredoxin, OsGRX6 affects hormone and nitrogen status in rice plants. Front Plant Sci. 2015;6:934.
56. Luo J, Huang S, Wang M, Zhang R, Zhao D, Yang Y, et al. Characterization of the transcriptome and proteome of *Brassica napus* reveals the close relation between DW871 dwarfing phenotype and stalk tissue. Plants. 2022;11:413.
57. Guo F, Hou L, Ma C, Li G, Lin R, Zhao Y, et al. Comparative transcriptome analysis of the peanut semi-dwarf mutant 1 reveals regulatory mechanism involved in plant height. Gene. 2021;791:145722.
58. Um TY, Hong SY, Han JS, Jung KH, Moon S, Choi B-S, et al. Gibberellic acid sensitive dwarf encodes an ARPC2 subunit that mediates gibberellic acid biosynthesis, effects to grain yield in rice. Front Plant Sci. 2022;13:1027688.
59. Que F, Wang Y-H, Xu Z-S, Xiong A-S. *DcBAS1*, a carrot brassinosteroid catabolism gene, modulates cellulose synthesis. J Agric Food Chem. 2019;67:13526–33.
60. Lu Q, Shao F, Macmillan C, Wilson IW, van der Merwe K, Hussey SG, et al. Genomewide analysis of the lateral organ boundaries domain gene family in Eucalyptus grandis reveals members that differentially impact secondary growth. Plant Biotechnol J. 2018;16:124–36.
61. Ren H, Willige BC, Jaillais Y, Geng S, Park MY, Gray WM, et al. BRASSINOSTEROID-SIGNALING KINASE 3, a plasma membrane-associated scaffold protein involved in early brassinosteroid signaling. PLoS Genet. 2019;15:e1007904.
62. Sakamoto T, Kawabe A, Tokida-Segawa A, Shimizu B, Takatsuto S, Shimada Y, et al. Rice CYP734As function as multisubstrate and multifunctional enzymes in brassinosteroid catabolism. Plant J. 2011;67:1–12.
63. Yang Z, Zhang C, Yang X, Liu K, Wu Z, Zhang X, et al. PAG1, a cotton brassinosteroid catabolism gene, modulates fiber elongation. New Phytol. 2014;203:437–48.
64. Ohnishi T, Nomura T, Watanabe B, Ohta D, Yokota T, Miyagawa H, et al. Tomato cytochrome P450 CYP734A7 functions in brassinosteroid catabolism. Phytochemistry. 2006;67:1895–906.
65. Chen Y, Dan Z, Gao F, Chen P, Fan F, Li S. Rice GROWTH-REGULATING FACTOR7 modulates plant architecture through regulating GA and indole-3-acetic acid metabolism. Plant Physiol. 2020;184:393–406.
66. Phillips KA, Skirpan AL, Liu X, Christensen A, Slewinski TL, Hudson C, et al. Vanishing tassel2 encodes a grass-specific tryptophan aminotransferase required for vegetative and reproductive development in maize. Plant Cell. 2011;23:550–66.
67. Yoshikawa T, Ito M, Sumikura T, Nakayama A, Nishimura T, Kitano H, et al. The rice FISH BONE gene encodes a tryptophan aminotransferase, which affects pleiotropic auxin-related processes. Plant J. 2014;78:927–36.
68. Lu G, Coneva V, Casaretto JA, Ying S, Mahmood K, Liu F, et al. OsPIN5b modulates rice (*Oryza sativa*) plant architecture and yield by changing auxin homeostasis, transport and distribution. Plant J. 2015;83:913–25.
69. Liu Y, Liu Y, He Y, Yan Y, Yu X, Ali M, et al. Cytokinin-inducible response regulator *SlRR6* controls plant height through gibberellin and auxin pathways in tomato. J Exp Bot. 2023;74:4471–88.
70. Lee K-H, Du Q, Zhuo C, Qi L, Wang H. LBD29-involved auxin signaling represses NAC master regulators and fiber wall biosynthesis. Plant Physiol. 2019;181:595–608.
71. Okushima Y, Fukaki H, Onoda M, Theologis A, Tasaka M. ARF7 and ARF19 regulate lateral root formation via direct activation of *LBD/ASL* genes in *Arabidopsis*. Plant Cell. 2007;19:118–30.
72. Okushima Y, Overvoorde PJ, Arima K, Alonso JM, Chan A, Chang C, et al. Functional genomic analysis of the AUXIN RESPONSE FACTOR gene family members in *Arabidopsis* thaliana: unique and overlapping functions of ARF7 and ARF19. Plant Cell. 2005;17:444–63.
73. Li W, Chu C, Li H, Zhang H, Sun H, Wang S, et al. Near-gapless and haplotype-resolved apple genomes provide insights into the genetic basis of rootstock-induced dwarfing. Nat Genet. 2024;56(3):505–16.

74. Wang T, Liu L, Wang X, Liang L, Yue J, Li L. Comparative analyses of anatomical structure, phytohormone levels, and gene expression profiles reveal potential dwarfing mechanisms in Shengyin bamboo (*Phyllostachys edulis* f. *tubaeformis*). IJMS. 2018;19:1697.
75. Park J-E, Kim Y-S, Yoon H-K, Park C-M. Functional characterization of a small auxin-up RNA gene in apical hook development in *Arabidopsis*. Plant Sci. 2007;172:150–7.
76. Spartz AK, Lor VS, Ren H, Olszewski NE, Miller ND, Wu G, et al. Constitutive expression of *Arabidopsis* SMALL AUXIN UP RNA19 (SAUR19) in tomato confers auxin-independent hypocotyl elongation. Plant Physiol. 2017;173:1453–62.
77. Spartz AK, Ren H, Park MY, Grandt KN, Lee SH, Murphy AS, et al. SAUR inhibition of PP2C-D phosphatases activates plasma membrane H+-ATPases to promote cell expansion in *Arabidopsis*. Plant Cell. 2014;26:2129–42.
78. Kim D, Langmead B, Salzberg SL. HISAT: a fast spliced aligner with low memory requirements. Nat Methods. 2015;12:357–60.
79. Li B, Dewey CN. RSEM: accurate transcript quantification from RNA-Seq data with or without a reference genome. BMC Bioinf. 2011;12:323.
80. Wang Z, Gerstein M, Snyder M. RNA-Seq: a revolutionary tool for transcriptomics. Nat Rev Genet. 2009;10:57–63.
81. Young MD, Wakefield MJ, Smyth GK, Oshlack A. Gene ontology analysis for RNA-seq: accounting for selection bias. Genome Biol. 2010;11(2):R14.
82. Huo F, Wang X, Han Y, Bai Y, Zhang W, Yuan H, et al. A new derivatization approach for the rapid and sensitive analysis of brassinosteroids by using ultra high performance liquid chromatography-electrospray ionization triple quadrupole mass spectrometry. Talanta. 2012;99:420–5.
83. Hellens RP, Allan AC, Friel EN, Bolitho K, Grafton K, Templeton MD, et al. Transient expression vectors for functional genomics, quantification of promoter activity and RNA silencing in plants. Plant Methods. 2005;1:13.
84. Lu S, Zhang Y, Zhu K, Yang W, Ye J, Chai L, et al. The citrus transcription factor CsMADS6 modulates carotenoid metabolism by directly regulating carotenogenic genes. Plant Physiol. 2018;176:2657–76.
85. Transcriptomic study of different tissues of mume 'Longyan' plant grafted on mume rootstock and peach rootstock. NCBI. 2024. https://www.ncbi.nlm.nih.gov/bioproject/?term=PRJNA1055178.
86. MTBLS10051: Metabolomics study of different tissues of mume 'Longyan' plant grafted on mume rootstock and peach rootstock (root) . EMBL-EBI MetaboLights. 2024. https://www.ebi.ac.uk/metabolights/editor/MTBLS10051/descriptors.
87. MTBLS10062: Metabolomics study of different tissues of mume 'Longyan' plant grafted on mume rootstock and peach rootstock (stem) . EMBL-EBI MetaboLights. 2024.https://www.ebi.ac.uk/metabolights/editor/MTBLS10062/descriptors.
88. MTBLS10083: Metabolomics study of different tissues of mume 'Longyan' plant grafted on mume rootstock and peach rootstock (leaf) . EMBL-EBI MetaboLights. 2024. https://www.ebi.ac.uk/metabolights/editor/MTBLS10083/descriptors.

Publisher's Note